WYDANIE 03 - STYCZEŃ, 2025

CZASOPISMO MEBUTRA

MEBUTRA

CZASOPISMO KATEDRY BUDOWNICTWA,
KATEDRY INŻYNIERII MECHANICZNEJ,
KATEDRY ELEKTROTECHNIKI I KATEDRY TRANSPORTU

"HOSE" PUMP - Test rig construction

Leakproof testing of plastic pipelines

The relationship between the type of structure and the number of construction disasters

The correlation between the population and number of construction disasters

Design and construction of a model of an undershot hydroelectric power plant

ANS
Akademia Nauk Stosowanych

ZESPÓŁ REDAKCYJNY

mgr inż. **Karolina Pikulik**
dr inż. **Jarosław Mikołajczyk**
Justyna Płociniczak

j.mikolajczyk@ans.pila.pl | wydawnictwo@ans.pila.pl

KOMITET NAUKOWY

RECENZENCI

Foreword

The year 2025 is already the third year when our University Journal "MEBUTRA" is published, which makes us extremely happy.
I sincerely encourage all our students, especially students of the Department of Mechanical Engineering, Department of Electrical Engineering, Department of Transport and Department of Civil Engineering to submit their papers as this journal is primarily dedicated to you, students of our Alma Mater. I also strongly encourage people who are members of the Student Research Groups of our university to write articles because the scientific achievements of these research associations are often very impressive.

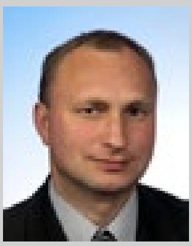

ON BEHALF OF THE EDITORIAL STAFF

dr inż. Jarosław Mikołajczyk

jmikolajczyk@ans.pila.pl

Spis treści

„HOSE” PUMP – TEST RIG CONSTRUCTION

inż. Rafał Kuliński

ORCID No.: 0009-0002-4808-7240; e-mail: rkulinski@interia.pl

Stanisław Staszic State University of Applied Sciences in Piła,

Department of Mechanical Engineering

1. Peristaltic pumps

A peristaltic pump, also known as a tube pump or hose pump, is classified as a positive-displacement pump with a rotary motion of the working element. It was created from the analysis of the functioning of the digestive system. Peristalsis causes the food to move. This observation made it possible to build a structure that works without valves, membrane or a piston. The working element is an impeller with rollers or slides pressing a flexible hose. The rotation of the impeller causes the liquid to be forced from the suction side to the discharge side (Fig. 1).

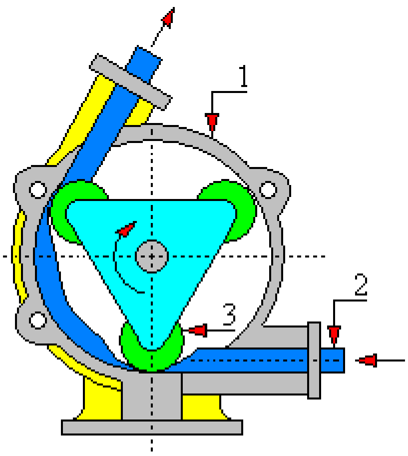

Fig. 1. Schematic diagram of a peristaltic pump with a three-arm impeller
1 – casing; 2 – flexible hose; 3 – roller compressing the flexible hose

The peristaltic pump is characterized by its efficiency in pumping liquids of high and low viscosity. The lack of seals and mechanical elements allows pumping abrasive and aggressive liquids. It is distinguished by its high self-suction capability. Thanks to dry operation, there is no need to fill the pump beforehand. The liquid is in contact only with the chemically resistant hose. The pump doses with high accuracy which is of great importance when pumping sterile liquids. It is efficient regardless of the pressure. Another advantage is full tightness and effective operation in opposite directions. The structure does not leak despite the lack of rotating seals. The peristaltic pump works gently. The simple design ensures cheap and easy maintenance. The only element that requires washing is the hose. Its cleaning is quick and thorough. The pump is universal. It can be used to pump completely different fluids. It also works well in the case of liquid and gas mixtures.

The disadvantage of the peristaltic pump is the unevenness of pumping. There is visible pulsation of the liquid which can only be removed with the help of a dampener. The working hose wears out quickly and requires frequent replacement. For this reason, the pump is rarely used for continuous operation. It does not work well when there is no possibility of systematically checking the wear of the hose. One of the limitations of the application is the use of solvents. The chemical reaction causes rapid degradation of the hose.

There are modern low-pressure hoses that are resistant to petroleum derivatives. However, this is a rarely used solution due to its high cost.

The advantages and development of production technology allow of many practical applications of peristaltic pumps. They have been used in hospitals and laboratories for many years. They enable the transfusion of infusion fluids and dialysis therapy. They are also used in the food and cosmetics industry. They pump thick juices and pastes. They are effective in pumping creams with coffee and peanut content. They transport emulsions regardless of their density and ability to foam. An interesting application is the dosing of lime milk. The lack of sealing ensures long operation without failures. Thanks to the operation in both directions it is possible to efficiently change the oil in the mechanisms of machines. The pumps are effective in pumping paints and glue. They are useful in the transport of waste and in sewage treatment plants. They facilitate the work of fire brigade units when evacuating leaks from tanks. They enable the pumping of ceramic mass. This liquid requires gentle pumping without aeration. Pumps are used in agriculture. They transport compost with sand, fertilizers and enzymes. They are used in the construction and printing industries.

2. Peristaltic pump hoses

The hose is the working section of the peristaltic pump. The material it is made of and its mechanical properties determine the pump's efficiency. Its selection depends on the type of pumped liquid. Individual hoses differ in chemical and mechanical strength. Other parameters include temperature resistance and sterilization possibility. Hoses differ in stiffness and certificates they hold. Their service life is influenced by the flexibility of the hose. It ensures quick recovery of shape after the roller has rolled over. Important features include resistance to cracking and abrasion. Thanks to chemical resistance, it is possible to pump various types of aggressive liquids. An important parameter when selecting a hose is the wall thickness. The internal diameter directly affects the efficiency of the hose. The correctly selected hose material determines the effective pumping of the medium. Santoprene hoses are characterized by very high durability and resistance to chemicals. They are used in the food and pharmaceutical industries. Viton hoses are characterized by resistance to temperature and weather conditions. They are non-flammable and stretchable. They are suitable for pumping hot oils, acids and greases. Neoprene hoses are used in general industry. They are resistant to ozone, abrasion and thermal radiation. Silicone hoses are universal and fulfill a function in many peristaltic pumps. Their properties include physiological indifference and elasticity. They are resistant to radiation, oxidation and temperature. The disadvantages of silicone hoses include shorter durability and lack of resistance to petroleum-derived compounds.

3. Design and construction of a hose pump

There are many existing design solutions for hose pumps, depending on their application. Most often, such designs are used either in medicine or in the chemical industry because of their specific features. Below, three solutions for the construction of hose pumps are developed and their advantages and disadvantages are characterized. From the above examples, one was selected for implementation, the most optimal one due to the existing possibilities of its realization.

As the first design of a hose pump, a hose pump with two compressing rollers (Fig. 2) placed in a rigid casing was developed. This type of solution ensures correct pump operation but only for one type of hose diameter. There can be many types of materials used to make hoses but all of them should have the same outer diameter, due to the lack of possibility of adjusting the arrangement of the hose compressing rollers. To drive this structure a continuously variable bevel gear transmission would be designed, which would significantly increase the weight of the entire structure. The advantage, however, is the simplicity of the construction and reliability of operation.

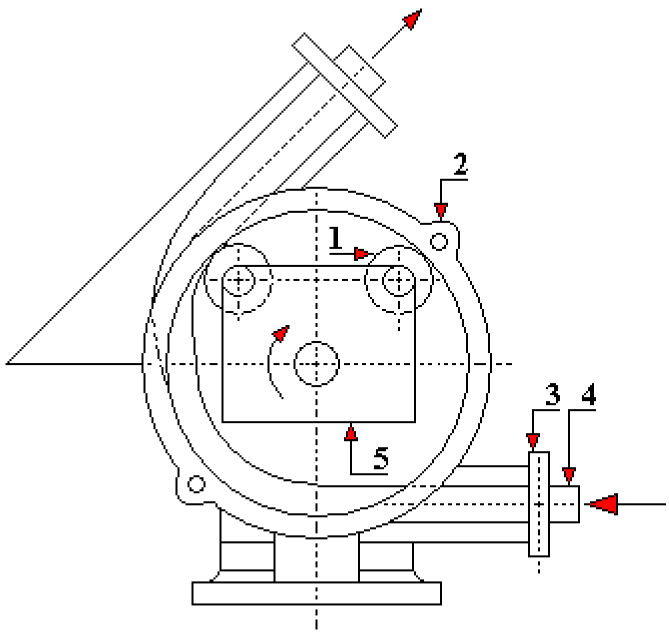

Fig. 2. Design No. 1 of a hose pump
1 – roller compressing the silicone hose; 2 – pump casing; 3 – connector; 4 – silicone hose; 5 – impeller fastening the compressing rollers

The second hose pump design, shown in Fig. 3, refers the existing structural solution of the hose pump used in flexible endoscope washers manufactured by Lancer [3, 4, 8, 18, 39, 45, 61]. In this type of pumps, a swing clamp is used, which allows of an easy and quick replacement of the hose that pumps the liquid, most often a washing and disinfecting fluid, highly aggressive to human skin. The pump is used to dose this agent during the washing process of flexible endoscopes after a given examination on a patient. The dimensions of this type of pump can be very small, there are even hose clamp pumps with external dimensions of approx. 60x60 mm. Stepper motors are used as the pump drive. The system uses a flow sensor that monitors the amount and speed of the flow of a given chemical agent. The entire system is controlled via a touch panel. The disadvantage of this solution is that the clamp has fixed dimensions because it is usually made of plastic. It is therefore impossible to change the size of the type of hose used to pump the liquid. Another disadvantage, as with all types of pumps of this type, is that the inner walls of the hose stick together which prevents the pumping of a given medium. Sometimes, the hoses have to be replaced even every three months. It is not difficult or expensive, but in the absence of this type of hose, the entire machine cannot work. Endoscopes usually have several channels inside, two, three or more, and each of them is connected to a different washing system [5, 15, 16, 19, 22, 27, 49]. In such solutions, only one endoscope can be washed at a time. Washing time is about one to two hours depending on the selected program and type of endoscope used. In the event of a washer failure, it is of course possible to wash the endoscopes manually, but there is no certainty that this will be done correctly, due to the specific structure of this type of medical constructions and its considerable length (over one meter including manual manipulators).

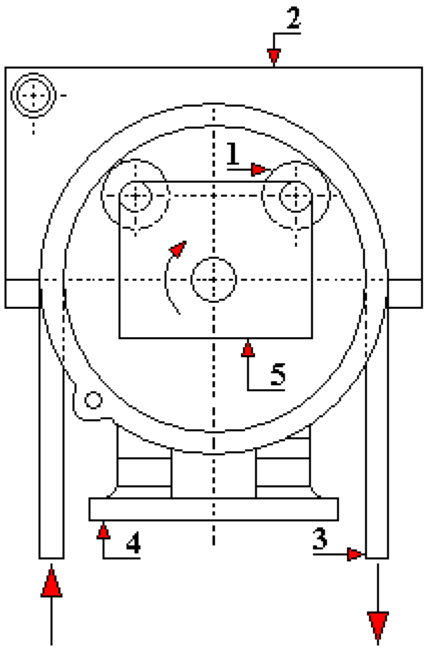

Fig. 3. Design No. 2 of a clamp hose pump
1 – roller compressing the silicone hose; 2 – swing clamp, pressing the pump casing against the rollers; 3 – silicone hose; 4 – pump casing; 5 – impeller fastening the compressing rollers

The third pump design is much more complicated technically than other designs (Fig. 4). To make it, elements obtained in an economic way were used, simply as waste from various types of electromechanical constructions. The casing of the machine (pump) is a steel table. On its upper plate, in the middle of which there is an opening through which the drive shaft of the electric motor passes, a steel ring with a roller mechanism is mounted. Rotary rollers (four pieces), pressing on the hose, are placed on the impeller. The impeller has slots in the shape of milled beans, which allows adjustment of the distance between the rollers. Thanks to this, it is possible to use hoses with a certain range of external diameters, which makes this device universal. Holes tangential to the ring are made in the steel casing (steel ring). This solution protects the hoses from bending and damage due to the collapse of the hose cross-section. Of course, making such holes is very difficult but it significantly extends the service life of applied pumping hoses. A frequency converter (inverter) is used to drive the electric motor enabling smooth change of the engine speed by changing the frequency of the supply current in the range from 0 to 50 Hz. Hose pumps operate at low rotational speeds, which is why it is important to ensure the lowest possible speeds and ability to control them. The inverter's operating parameters can be changed manually from the control panel, or programmatically from a computer using a free application provided by the manufacturer. Such design solutions are currently widely available and convenient both due to the low costs of frequency converters, both new and recycled, and due to the reliability of operation and ease of use. Therefore, it was decided to implement this design solution of the hose pump, despite certain technical difficulties related to its construction [1, 2, 5, 10, 15, 33, 34].

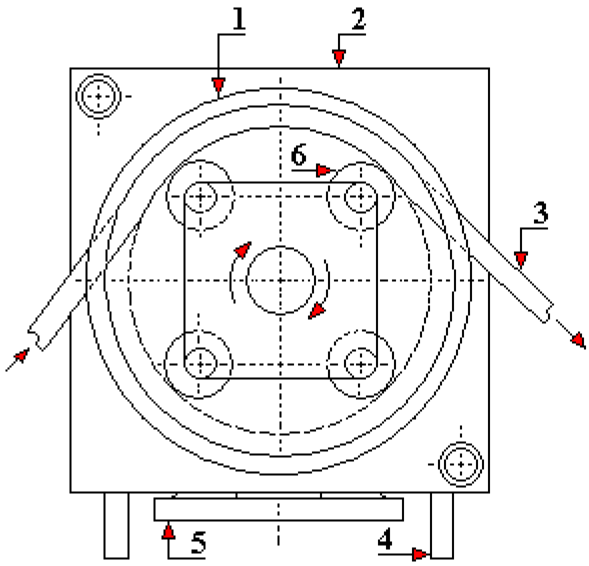

Fig. 4. Design No. 3 of a hose pump with adjustable compressing roller distances
1 – steel ring attached to the base table; 2 –base table; 3 – silicone hose; 4 – flat bars designed for mounting additional equipment, according to the user's needs; 5 – frequency converter that powers and controls the operation of the electric motor, located at the bottom of the table; 6 – roller pressing the hose to the steel ring

Fig. 5. View of the spacer that determines the position of the hose. The outer diameter of the spacer is Ø220mm, the inner diameter is Ø205mm, while the thickness and height are b=h=18mm. The material used is Teflon.

Fig. 6. View of the used Leroy Somer frequency converter (inverter). Designations of control ports: 01- minimum speed [Hz]; 02- maximum speed [Hz]; 03 – acceleration value [sec/100Hz]; 04 – delay value [sec/100Hz]; 05 – determination of the gradual speed difference; 06-rated motor current [A]; 07 – rated motor speed [rpm]; 08-rated motor voltage [V]; 09- determination of the power factor value (cosφ); 10 – available parameters. Current ports: L1 – first phase; L2/N – second phase or neutral conductor (optional); PE- protective conductor; U, V, W – motor connection + grounding.

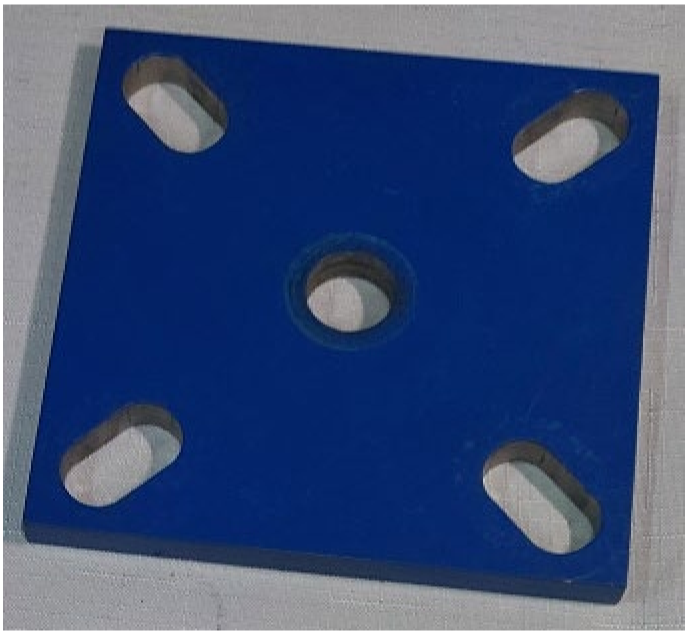

Fig. 7. View of the plate (2 pieces) securing the impeller. Plate dimensions: 130x130x11mm. The diameter of the central hole is Ø20mm. The longitudinal millings ("beans") have the following dimensions: 17x29mm

Fig. 8. View of the impeller distance sleeve. The sleeve dimensions are as follows: Ø22x2.5x31mm

Fig. 9. Arrangement of the spacer ring and the plate securing the impeller to the table base

Fig. 10. View of the arrangement of the drive rollers

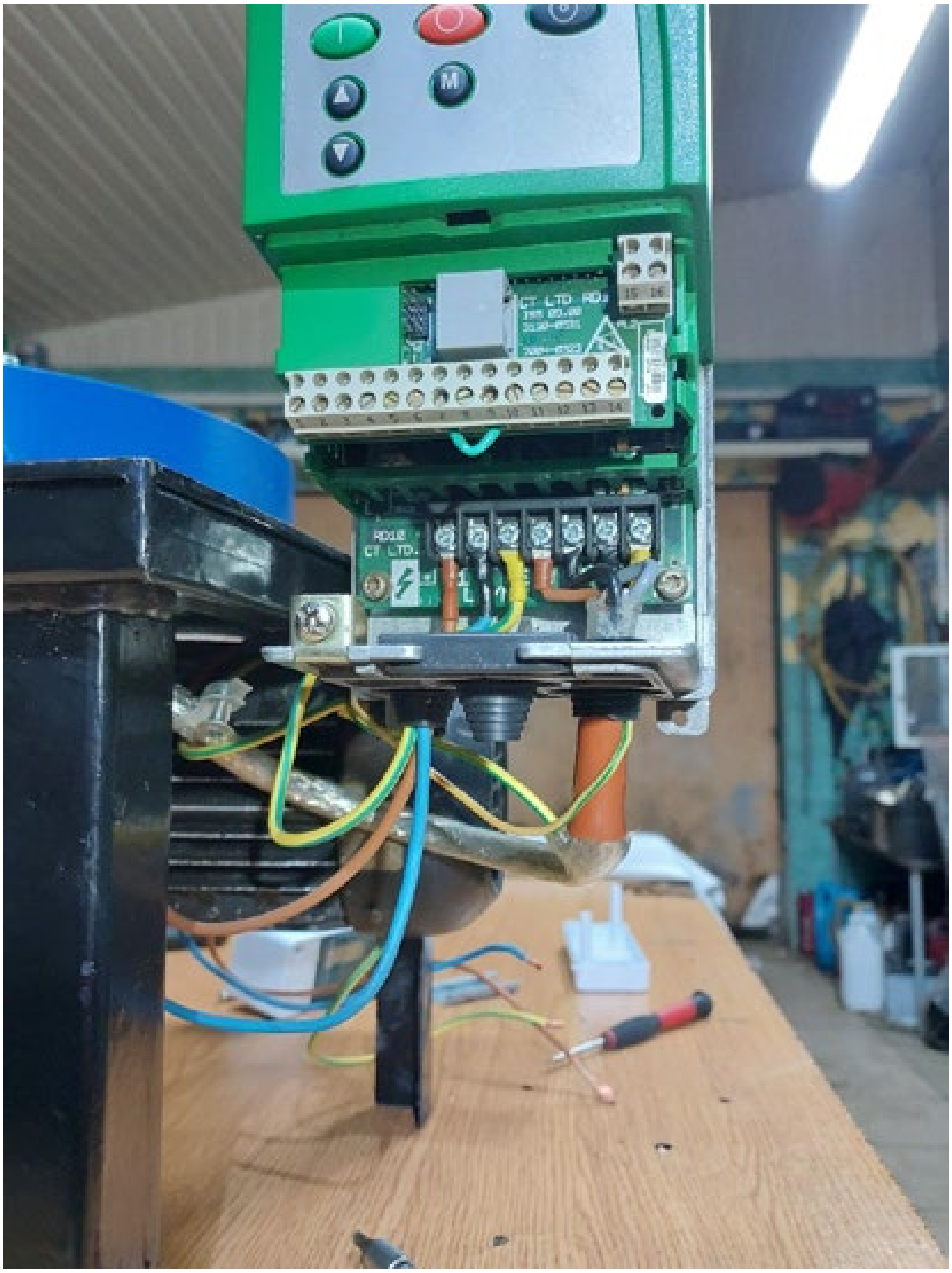

Fig. 11. Connecting power and control cables to a Leroy Somer frequency converter

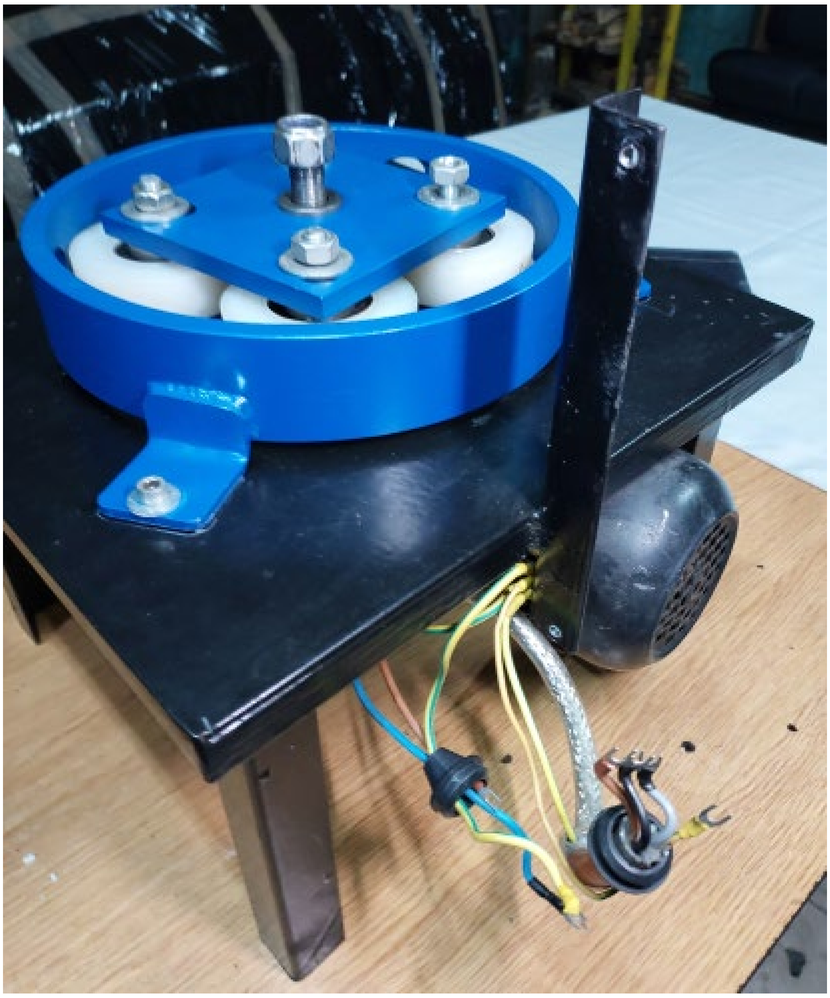

Fig. 12. View of the test rig during final assembly works. Visible is the table that constitutes the casing of this test rig. The drive motor is located under the table. The pump's working raceway is mounted on the table. The frequency converter will be attached to the side angle bracket, acting as a frame.

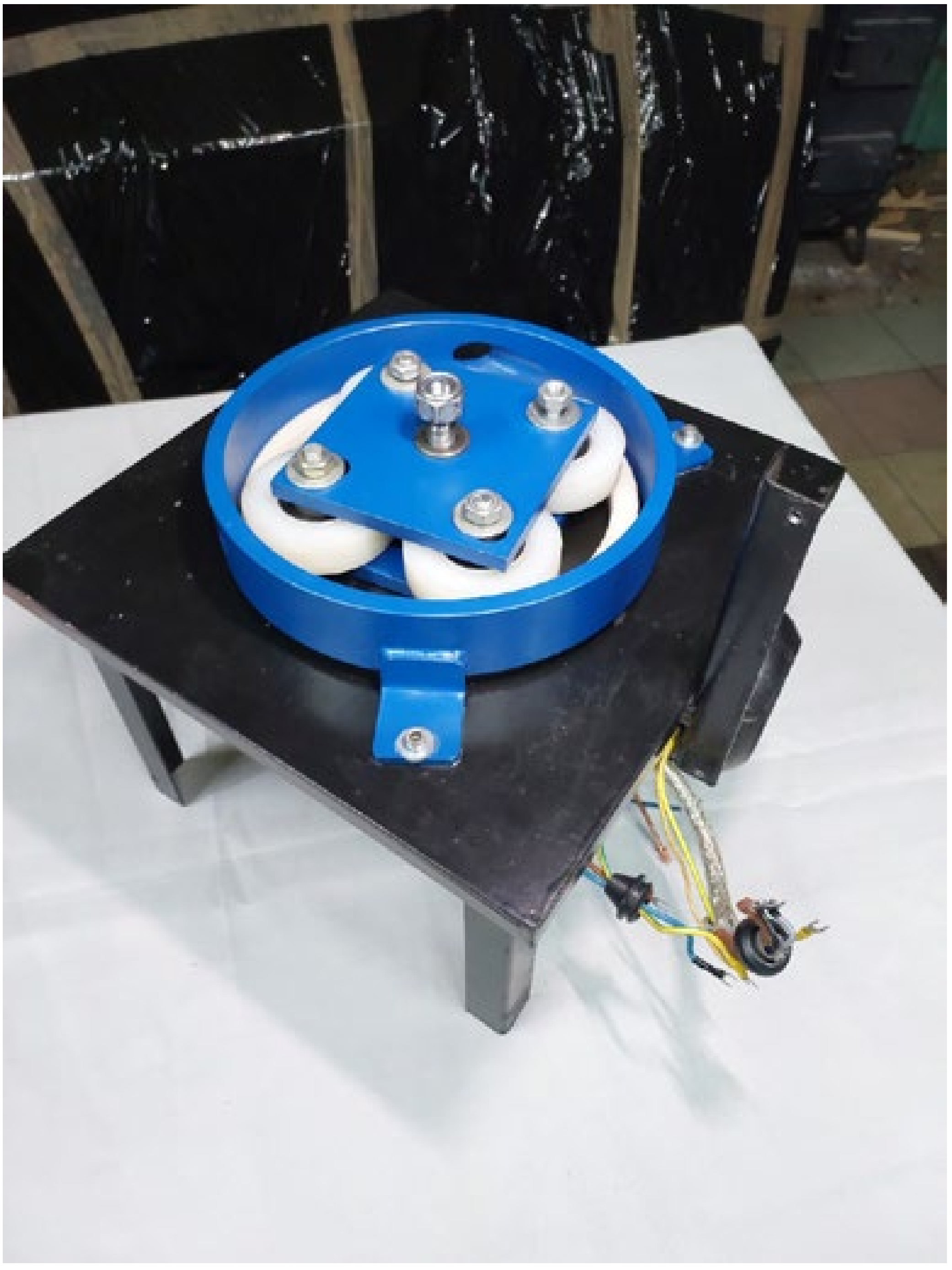

Fig. 13. General view of the hose pump test rig during assembly

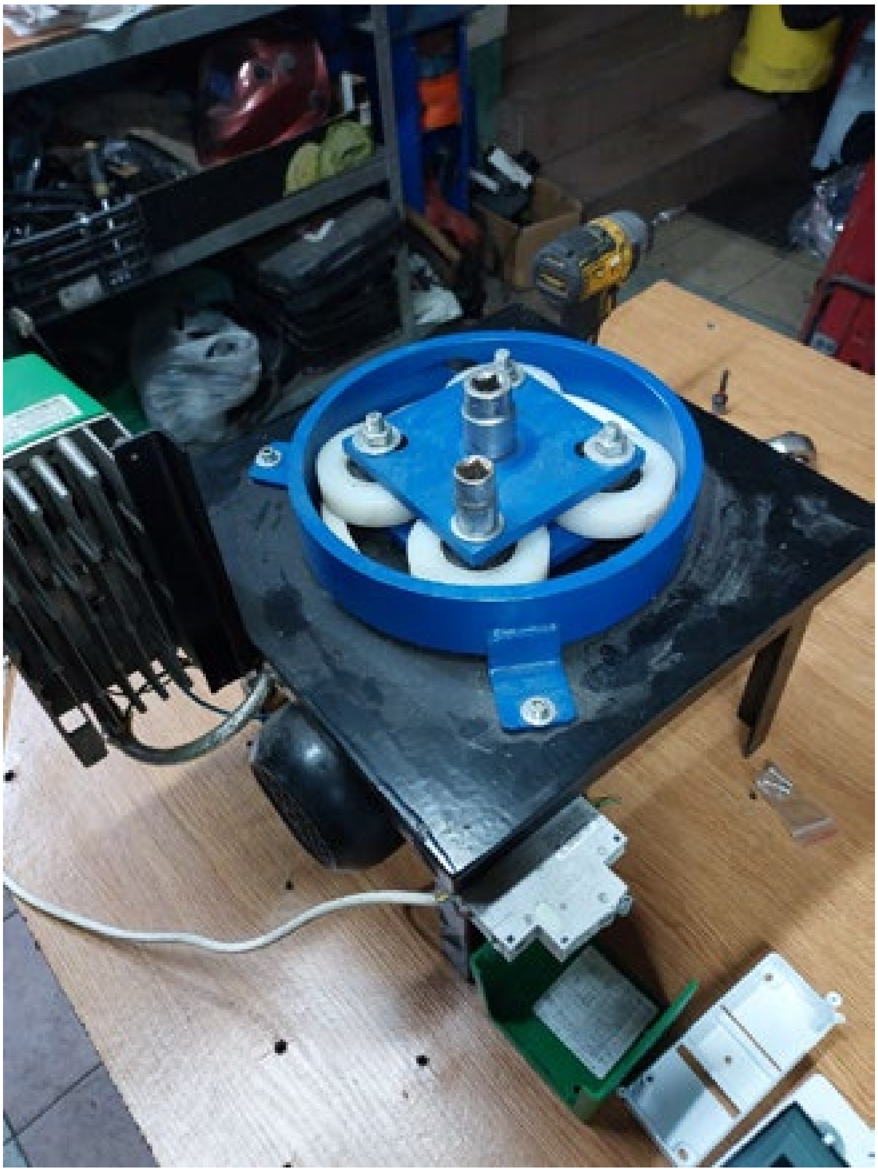

Fig. 14. Top view of the hose pump test rig

Fig. 15. Standardized machine elements used to secure the raceway to the table. Flat washers Ø6xØ12x1.5mm (8 pieces). M6x20 screws (4 pieces) and self-locking nuts for them (4 pieces).

Fig. 16. Standardized machine elements used to secure the frequency converter as well as control and power cables. M5x12 screws with cheese head. M5x7 screws with Phillips head and M5x11 screws also with Phillips head. Flat washers Ø6xØ12x1.5mm

Fig. 17. View of the completed raceway (steel ring). The inner diameter is Ø235 mm, the outer diameter is Ø245 mm, the total height of the track is h_{total} = 53 mm, the ring height is h = 45 mm. Two tangential holes with a diameter of Ø30mm are made in the ring, intended for the mounting of silicone hoses

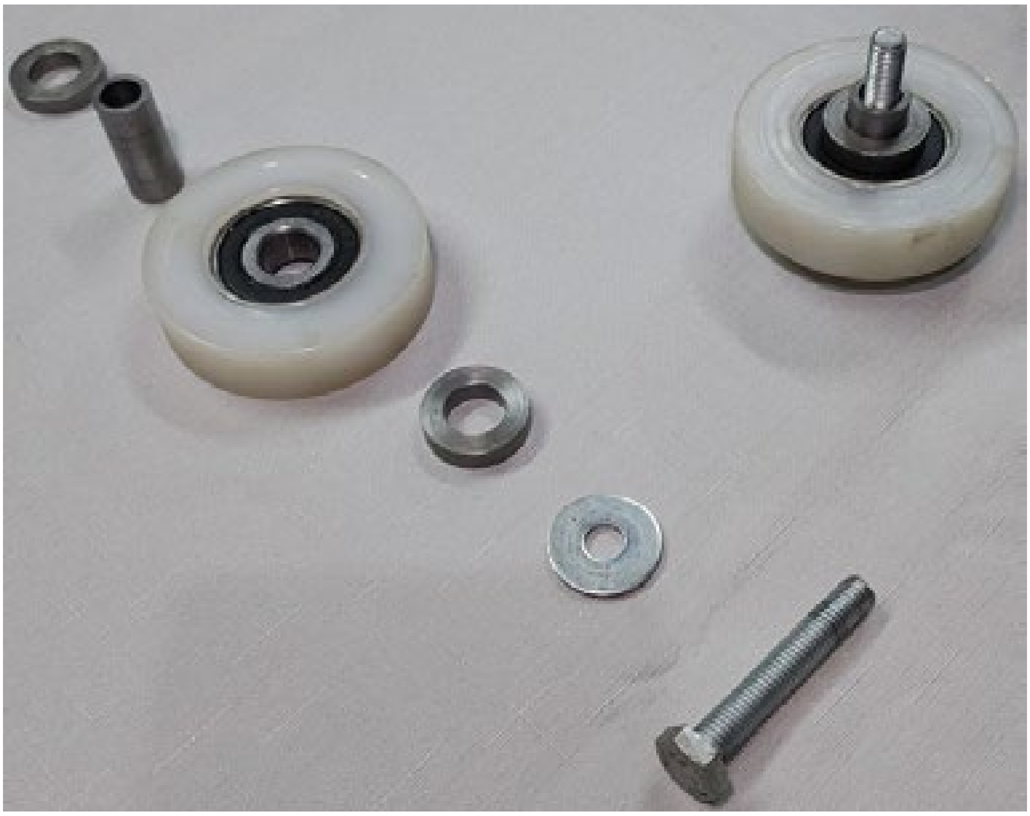

Fig. 18. Components of rollers (4 pieces) compressing the hoses. Locating and fastening parts

Fig. 19. View of the roller compressing the silicone hoses. The outer diameter of the roller is Ø80mm, and its height is h=20mm. The rollers are made of Teflon. A 6303RS type rolling bearing with double-sided seal is used.

Fig. 20. Examples of silicone hoses with an internal diameter of Ø10 mm adapted to work in this pump design

4. Summary

The designed and implemented construction of the hose pump enables pumping of practically any type of medium, depending on the type of hose materials used. The frequency converter used in the drive construction ensures smooth change of the impeller rotational speed in a wide range, depending on the user's needs. The construction also makes it possible to use hoses of different diameters thanks to the possibility of changing the location of the wheels, the compressing rollers. Of course, there is a possibility of further extension and improvement of this construction, e.g. by using compressing rollers of different diameters or different cross-sectional profile, or mounted on flexible connections, thanks to this the construction enables further changes in its structure, which is its undoubted advantage.

5. Literature

1. Bochenek A.: *Elementy mechaniki pękania*. Politechnika Częstochowska, Częstochowa, 1998.
2. Brzoska Z.: *Wytrzymałość materiałów.* PWN, Warszawa, 1979.
3. Chmielewski H.: *Układ SI*. WSiP, Warszawa, 1979.
4. Czajkowski J.: *Elementy przyrządów precyzyjnych*. WSiP, Warszawa, 1983.
5. Dacko M., Borkowski W., Dobrociński S., Niezgoda T., Wieczorek M.: *Metoda elementów skończonych w mechanice konstrukcji*. Wydawnictwo Arkady, Warszawa, 1994.
6. Dąbrowski Z., Maksymiuk M.: *Wały i osie*. PWN, Warszawa, 1984.
7. Dietrych M., Szopa T.: *O optymalizacji zabezpieczenia maszyny*. Arch. Bud. Masz., 1976/4.
8. Dobrowolski Z.: *Podręcznik spawalnictwa*. WNT, Warszawa, 1978.
9. Gabryelewicz F.: *Części maszyn dla samouków*. Część I i II. PWSZ, Warszawa, 1964.
10. Gołaski L.: *Elementy doświadczalnej mechaniki pękania*. Politechnika Świętokrzyska, Kielce, 1994.
11. Horwatt W., Bartoszewicz J.: *Podstawy konstrukcji mechanicznych dla elektryków*. WNT, Warszawa, 1971.
12. Firkowicz S.: *Statystyczne badanie wyrobów*. WNT, Warszawa, 1970.
13. Fraenkel P.L.: *Water lifting. Food and Agriculture Organization Of The United Nations*. Rome 1986.
14. Janiak M., Krzyżaniak G.: *Urządzenia mechaniczne w inżynierii środowiska*. Część II. Wydawnictwo Politechniki Poznańskiej, Poznań 1995.
15. Jędrzejewski J.: *Mechanika układu korbowego*. WKŁ, Warszawa, 1979.
16. Kacperski T.: *Problemy odkształceń, tolerancji i luzów w maszynach*. Wydawnictwo Politechniki Warszawskiej, Warszawa, 1978.
17. Kapkowski J., Słowikowska I., Stupnicki J.: *Badanie naprężeń metodą elastooptycznej warstwy powierzchniowej*. PWN, Warszawa, 1986.
18. Kijewski J., Miller A., Pawlicki K., Szolc T.: *Maszynoznawstwo*. Wydawnictwa Szkolne i Pedagogiczne, Warszawa, 1993.
19. Kiliński A.: Definicje opisowo-analityczne i wartościująco-normatywne podstawowych pojęć teorii niezawodności. Prakseologia, z. 38, 1971r.
20. Kocańda S., Szala J.: *Podstawy obliczeń zmęczeniowych*. PWN, Warszawa, 1985.
21. Kocańda S.: *Zmęczeniowe pękanie metali*. Wyd. 3, WNT, Warszawa, 1985.
22. Kopociński B.: *Zarys teorii odnowy i niezawodności*. PWN, Warszawa, 1973.
23. Korewa W., Zygmunt K.: *Podstawy konstrukcji maszyn*, cz. 2, WNT, Warszawa, 1973.
24. Kułakowski J.: *Rysunek techniczny*. WSiP, Warszawa, 1976
25. Neimitz A.: *Mechanika pękania*. PWN, Warszawa, 1998.
26. Leyko J.: *Mechanika ogólna*, t. 1: Statyki i kinematyka, PWN, Warszawa, 1979.
27. Leyko J.: *Mechanika ogólna*, t. 2: Dynamika, PWN, Warszawa, 1979.
28. Lipka J.: *Wytrzymałość maszyn wirnikowych*. WNT, Warszawa, 1967.
29. Lipski J.: *Napędy i sterowania hydrauliczne*. Wydawnictwo Komunikacji i Łączności, Warszawa, 1981.
30. Łazarkiewicz S., Troskolański A.: *Pompy wirowe*. Wyd. II, WNT, Warszawa, 1968.
31. *Łożyska toczne. Katalog*. Wydawnictwa przemysłu Maszynowego, Warszawa, 1982.
32. Łukasiewicz S.: *Obciążenia skupione w płytach, tarczach i powłokach*. PWN, Warszawa, 1976.
33. Markusik S.: *Sprzęgła mechaniczne*. WNT, Warszawa, 1979.
34. Michałowska J.: *Paliwa, oleje i smary*. WKiŁ, Warszawa, 1973.
35. Michałowski M., Strokowski M.: *Automatyka i urządzenia kontrolno-pomiarowe*. PWSZ, Warszawa, 1967.
36. Miernicki S.: *Pasowania i pomiary*. PWSZ, Warszawa, 1969.
37. Muszyński W.: *Wykłady elementów maszyn*. Cz. I. PWT, Warszawa, 1951.

38. Müller L.: *Przekładnie zębate. Projektowanie*. WNT, Warszawa, 1979.
39. Müller L.: *Przekładnie obiegowe*. WNT, Warszawa, 1979.
40. Ochęduszko K.: *Koła zębate*. T. 1 i II, WNT, Warszawa, 1976.
41. Osiński Z.: *Teoria drgań*. PWN, Warszawa, 1978.
42. Parszewski Z.: *Teoria mechanizmów i maszyn*. WNT, Warszawa, 1976.
43. Piwowar S.: *Spawanie i zgrzewanie elektryczne*. PWSZ, Warszawa, 1966.
44. Pluta M.: *Holografia – podstawy fizyczne, teoria i zastosowanie*. PWN, Warszawa, 1980.
45. Pokutycki J.: *Podstawy automatyki*. PWSZ, Warszawa, 1968.
46. *Poradnik inżyniera mechanika*. Praca zbiorowa. Wydawnictwa Naukowo-Techniczne, Warszawa, 1968.
47. *PN-90/B-03200*: *Konstrukcje stalowe. Obliczenia statyczne i projektowanie*. Wydawnictwa Normalizacyjne, Warszawa, 1980.
48. Pułaczewski J.: *Automatyka*, PWSZ, Warszawa, 1969.
49. Ratyński J.: *Projektowanie konstrukcji metalowych*. PWSZ, Warszawa, 1970.
50. Rumszyński L.: *Matematyczne opracowanie wyników eksperymentalnych*. WNT, Warszawa, 1973.
51. Rutkowski A., Orlik Z.: *Części maszyn*, cz. II, WSiP, Warszawa, 1981.
52. Rutkowski A., Stępniewska A.: *Zbiór zadań z części maszyn*. WSiP, Warszawa, 1984.
53. Surowiak W.: *Nowe konstrukcje i metody obliczeń elementów maszynowych*. WNT, Warszawa, 1963.
54. Surowiak W.: *Części maszyn*. PWSZ, Warszawa, 1970.
55. Surowiak W., Chudzyńki S.: *Tworzywa sztuczne w budowie maszyn*. WNT, Warszawa, 1971.
56. Stępniewski M.: *Pompy*. Wydawnictwo Naukowo-Techniczne, Warszawa 1985.
57. Stryczek J.: *Koła zębate maszyn hydraulicznych*. Oficyna Wydawnicza Politechniki Wrocławskiej, Wrocław, 2007.
58. Stryczek J., Stryczek S.: *Pompy zębate – zarys historii*. Część 1 – Sterowanie i Napęd Hydrauliczny 2/1994, Część 2 – Sterowanie i Napęd Hydrauliczny 3/1994
59. Stybulski W.: *Przetworniki tensometryczne, konstrukcja, projektowanie, użytkowanie*. WNT, Warszawa, 1971.
60. Szablowski K.: *Pompy wyporowe*. PWN, Łódź-Warszawa-Kraków, 1964.
61. Szopa T.: *Wprowadzenie w problematykę bezpieczeństwa*. W: Bezpieczeństwo człowieka we współczesnym świecie. Wyd. Inst. Prob. Współcz. Cywilizacji, Warszawa, 1998.
62. Tryliński W.: *Drobne mechanizmy i przyrządy precyzyjne*. WNT, Warszawa, 1961.
63. Zatyka H.: *Spawanie wiązką elektronów*. WNT, Warszawa, 1986.
64. Zimmermann R.: *Pomiary drgań i naprężeń metodami elektrycznymi*. PWR, Warszawa, 1959.

LEAKPROOF TESTING OF PLASTIC PIPELINES

dr inż. Wiktor Kupraszewicz
ORCID No.: 0000-0001-6081-8793; e-mail: wkupraszewicz@ans.pila.pl
Stanisław Staszic State University of Applied Sciences in Piła, Poland
Department of Mechanical Engineering

In recent years, thanks to many investment programs implemented under European Union programs aimed at improving the poor supply of water and sewage to cities and villages, many investments have already been made and will be launched to improve this situation. A variety of water pipe designs, especially in terms of materials, poses a major challenge to investors, designers, contractors and operators at all stages of project implementation. The leakproof test of a plastic pipeline is the result of the quality of the tasks performed, provided that it is performed correctly, taking into account the viscoelastic properties of materials used to produce the pipes.

1. INTRODUCTION

After many years of experience with polymer materials, as practice shows, tightness testing of plastic pipelines should be carried out in accordance with the requirements taking into account the characteristic features of a specific material solution. At the same time, attention should be paid to the fact that the leakproof test criteria for different pipe construction materials had a tendency to get shorter e.g. the test duration. It should also be emphasized that other criteria used during the testing were "fuzzy", which resulted in the fact that reports and even works discussing the acceptance conditions were characterized by general statements, e.g. about the test lasting several hours or whether the test pressure should not decrease within 30 minutes. In order to eliminate the subjectivity of the evaluation of pipeline leakproof test results and at the same time improve the quality of their performance, PN-B-10725 standard was issued in 1997: December 1997 (withdrawn on 10 September 2012) and PN-EN 805 standard: December 2002, (published on 31 December 2002) which aimed at organizing and clearly defining the criteria in this area being in practice variously observed and interpreted in many different ways. Because this paper has its limits of volume it does not include other, no less important, leakproof test procedures resulting from other standards applied to plastic pipes.

2. STATE OF NORMATIVE REGULATIONS

In the scope of leakproof tests of plastic pipelines the standard currently in force in Poland is the Polish Standard PN-EN 805 established by the Polish Committee for Standardization on 31 December 2002. However, both standards may continue to be applied, but the withdrawn one covers external cables (requirements and testing) and the second one covers requirements for external systems and their components. The fundamental differences in the application of the above-mentioned standards result from their scope, as shown in Fig. 1.

[1] Chapter 1. Introduction. 1.1. Scope of the standard, page 2. PN-B-10725: December 1997 and Chapter 1. Scope of the standard, page 6. PN-EN 805: December 2002.

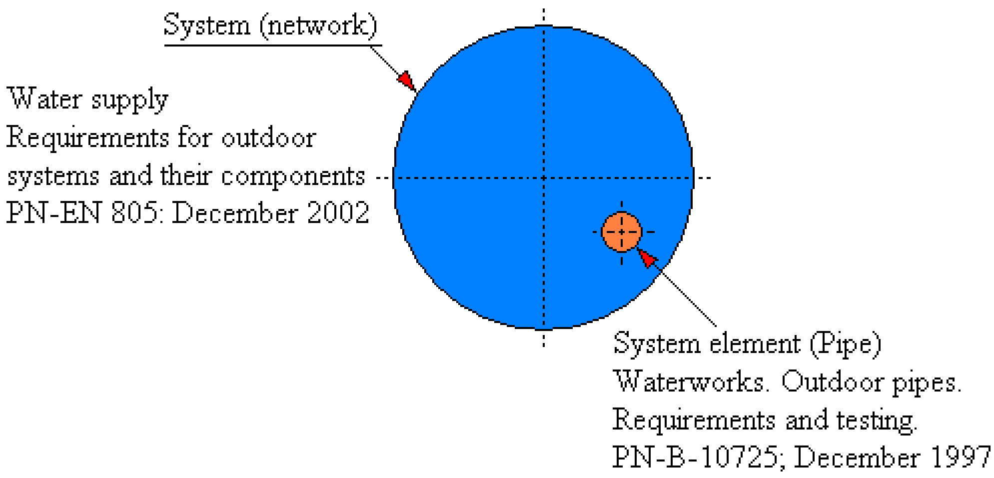

Figure 1. Scope of application of standards applicable to leak testing

The PN-B-10725 standard specifies the requirements and tests for partial and final technical acceptance of water pipes made of steel, cast iron and polyester or epoxy resins with glass fibre reinforcements and other plastics that have a certificate or declaration of conformity with the requirements of Polish Standards or technical approvals. And the PN-EN 805 standard in its scope refers to general requirements for external water supply systems (see Fig. 2) including main water pipes and connections, network tanks and other devices, and raw water pipes, excluding water treatment plants and water intakes.

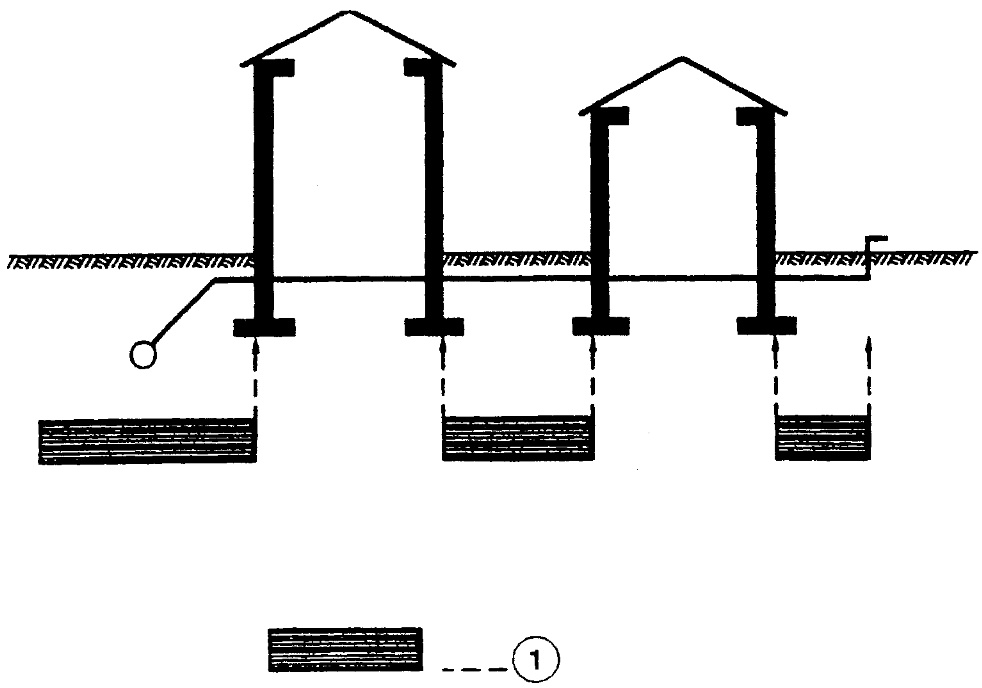

Figure 2. Scope of application of the PN-EN 805 standard: December 2002 [6]
1 - area of application

The fundamental differences presented above regarding the scope and area of application of the above standards may result in some freedom, especially when it comes to tests carried out partially, i.e. on pipeline sections. A clear solution to this fundamental issue is contained in the

European Pre-Standard ENV 1046:2001; its Polish version was published in 2007 as PN-ENV 1046: April 2007 and it was withdrawn without replacement on 8 April 2016.

In the cited standard, in chapter 8, Inspection and testing, on page 35, in subchapter 8.2.1. Pressure tests, it is clearly stated that the pressure test (tightness test) shall be carried out in accordance with the relevant European Standard(s). This condition is met only by Polish standards, previously adopted on a discretionary basis, based on European standards. The PN-EN 805 standard, which is clear from its marking, is such a standard and that is why it is the only one that should be used to test the tightness of plastic pipelines laid in the ground. However, in the case of a withdrawn and not replaced standard, the Polish Committee for Standardization (PKN) does not state in the additional information why the standard was withdrawn without replacement. At the same time, PKN specifies on its website what the standard is. A standard is a document adopted by consensus and approved by an authorized organizational unit (Technical Committee KT), establishing – for common and repeated use – principles, guidelines or characteristics relating to various types of activities or their results and aiming to achieve an optimal degree of order within a specific scope. For almost 50 years a mandatory system was in force in Poland, typical of a centrally controlled economy, which resulted in that the obligation to apply standards has become deeply embedded in the consciousness of the entire society. The information that the application of Polish Standards is voluntary is often still surprising, though 22 years after the introduction of this voluntary system there are fewer and fewer such comments made. Much less is known about what the voluntary standardization system brings, apart from the voluntary nature of applying standards, and these are more significant changes in relation to the mandatory system, especially for entrepreneurs. The system gives them many more opportunities and benefits which they are often not aware of.

Coming back to the issue of leakproof testing, the fundamental differences result from the basic pipe model which in the case of the basic material being a polymer material gives this structure flexibility, the so-called flexible pipes which can change their volume[2] significantly under the influence of internal or external pressure.

3. FLEXIBLE PIPE AND OTHER POLYMER PIPE CONSTRUCTIONS

According to PN-EN 805: December 2002 and requirements specified therein, the standard applies to:

- designing and building new water supply systems,
- expansion of the existing water supply system over a large area, creating a separate section,
- significant modification and/or modernization of existing water supply systems.

At the same time, the standard states that it is not recommended to make changes to existing water supply systems in order to meet the requirements of this standard, provided that there is no significant deterioration in water quality, safety, reliability and completeness of the system.
The presence of various plastic materials used in the production of pipes has been taken into account in the basic division of pipes as a basic element of the system. Depending on the load-bearing capacity we have the following pipe types:

- rigid pipe – a pipe whose load-bearing capacity is limited by breaking without significant deformation of the cross-section, the so-called rigid behaviour.
- semi-rigid pipe – a pipe whose ability to carry a load is limited either by deformation (overload), so-called elastic behaviour, or breaking, so-called rigid behaviour.
- flexible pipe – a pipe whose load-bearing capacity is limited by deformation (deflection and/or deformation of the cross-section), under a load equal to the design limit value, without breaking or tearing, so-called elastic behaviour.

A fundamental question must be asked: Are all plastic pipes flexible pipes (structures)? If not, which are and which are not flexible structures? What criteria determine this? The answer to these

[2] Bolt A., Suligowski Z.: „Próby szczelności rurociągów ciśnieniowych z tworzyw polimerowych", INSTAL 7-8/2007 rok.

questions is not that simple. It is included in the individual standards provided for given solutions and due to the limited volume of this paper it is not discussed in detail. An extreme case of such resistance is shown in Fig.3.

Figure 3. Example of a flexible pipe

The example (Fig. 3) shows that in the presented case the load-bearing capacity was maintained even when the design limit value was significantly exceeded, without any breakage, which fully confirms the elastic behavior of the manufactured pipe. Of course, the presented case was performed in laboratory conditions and fully confirmed the behavior of flexible pipes laid in the ground, as shown in Fig. 4. It should be noted here that the manufactured polymer pressure pipes will be flexible pipes, according to the definition adopted above, only if they meet all the requirements set by standards or national technical assessments - KOT (formerly technical approvals - AT). As a result of failure to meet, or questionable compliance with, certain quality requirements, there may also be cases in the production process where the pipes are semi-rigid, which - in the case of careless or even standard installation of the pipeline in the ground - may lead to significant damage to the pipeline already during the pressure test. The cause of this damage will be significant maximum deflections occurring after the pipeline has been laid (Fig. 4).

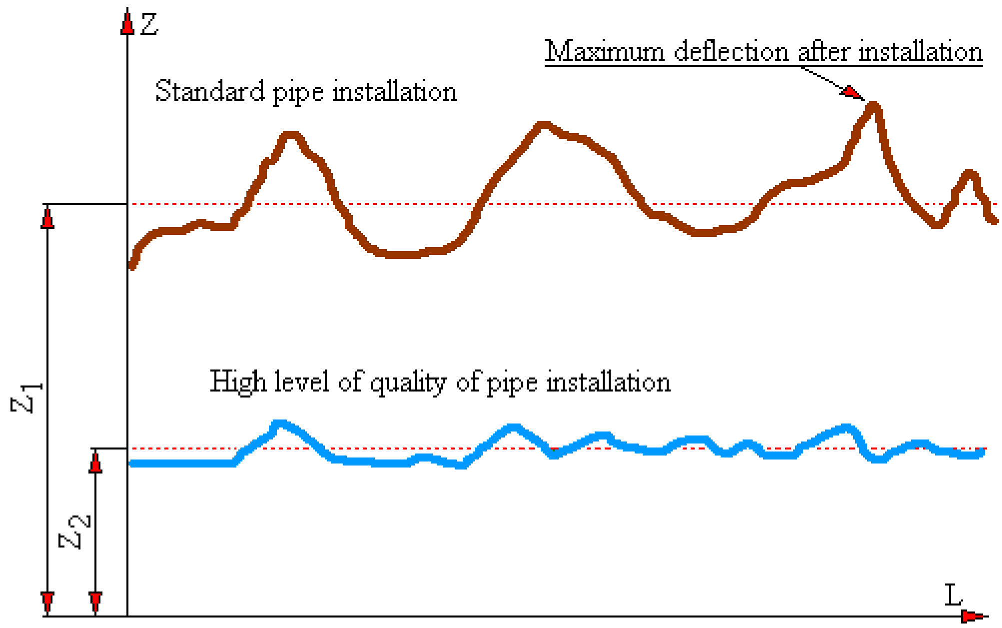

Figure 4. Typical changes in Z deflection along the L pipeline for two levels of laying quality [7]
Z_1 and Z_2 – average deflection after laying

The changes in deflection reflect the different support and the different effects of external loads on the pipe.

The results of the European research project "Design of underground thermoplastic pipelines" carried out by TEPPFA[3] and APME[4] several years ago have shed light and gave valuable results on the issue of designing pipelines made of thermoplastics (most often PVC, PE, PP) laid in the ground and their interaction with the ground medium. The influence of individual arrangement parameters and applied construction solutions on the deflection value was also determined:

- assembly conditions – 80%,
- pipe laying depth – 15%,
- pipe circumferential stiffness – approx. 3,5%,
- pipe material – approx. 1,5%.

The above division shows that the installation conditions, careful preparation and subsequent installation of the plastic pressure pipeline will mainly affect the pipe's behavior under the influence of external and internal loads, thus the operational reliability of the pipeline.

[3] European Plastic Pipes and Fittings Manufacturers Association
[4] European Plastics Manufacturers Association

4. PRESSURE TEST

According to the standard PN-ENV 1046: April 2007 (withdrawn without replacement on 08 April 2016), before carrying out pressure tests make sure that the pipeline, in particular the bends and thrust blocks and other fittings, are designed to withstand the forces caused by the test pressure. This standard requires that the test be carried out in accordance with the relevant European standard(s). In 2018, the standard PN-C-89224:2018-03 was introduced, Thermoplastic piping systems - External non-pressure and pressure systems for water transmission, drainage and sewage made of unplasticized poly(vinyl chloride) (PVC-U), polypropylene (PP) and polyethylene (PE) - Technical conditions for installation and acceptance. The standard was developed by the Technical Committee KT 140, in cooperation with KT 278, for Water and Sewage Systems. This standard specifies the technical conditions for the installation and acceptance of thermoplastic piping systems made of unplasticized poly(vinyl chloride) (PVC-U), polypropylene (PP), and polyethylene (PE) intended for underground, external pressure and non-pressure networks, including water supply networks, in accordance with PN-EN 805, pressure sewerage systems in accordance with PN-EN 1671, vacuum sewerage systems in accordance with PN-EN 1091 and gravity drainage and sewerage networks in accordance with PN-EN 476 and PN-EN 752. This standard applies to thermoplastic piping systems with nominal sizes up to and including DN 3000. One can assume that this standard filled the gap that emerged after the withdrawal of the pre-standard PN-ENV 1046.

The PN-EN 805:December 2002 standard specifies detailed requirements for the installation and testing of pipelines made of plastics. The scope of requirements implemented during the design and installation works is shown in Fig.5.

[3] Europejskie Stowarzyszenie Producentów Rur i Kształtek z Tworzyw Sztucznych
[4] Europejskie Stowarzyszenie Producentów Tworzyw Sztucznych

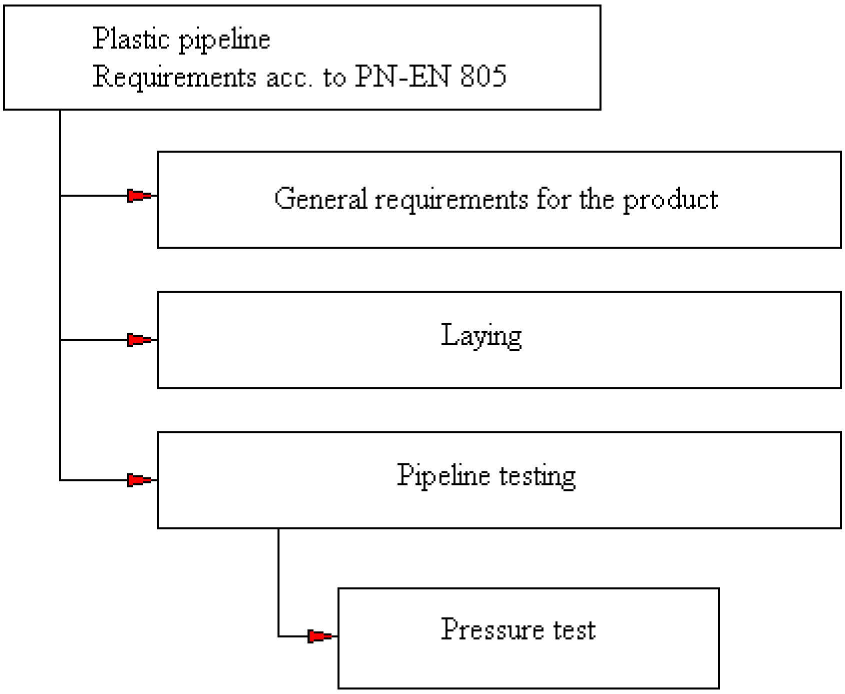

Figure 5. Requirements of the PN-EN 805 standard: December 2002

The pressure test should be carried out on the entire pipeline, or if this is not possible, it should be tested in sections. Before starting the tests, all elements (debris and foreign objects) must be removed from the pipeline. The tested section should be filled with water slowly and all air-venting devices should be open and properly vented prior to the test. Air should be removed from the pipeline as much as possible. Filling should be started, if possible, at the lowest point in the pipeline and in such a way that no siphon is formed below the filling point and that air escapes through the air vents..
The basic pipeline inspection consists of a pressure test which is carried out according with three basic stages. This procedure is performed regardless of the type of pipes and materials used. The test procedure should be defined by the designer and should include three stages (Fig. 6): preliminary test, pressure drop test and main pressure test, as specified in Annex A.27 of the previously mentioned standard PN-EN 805: December 2002.

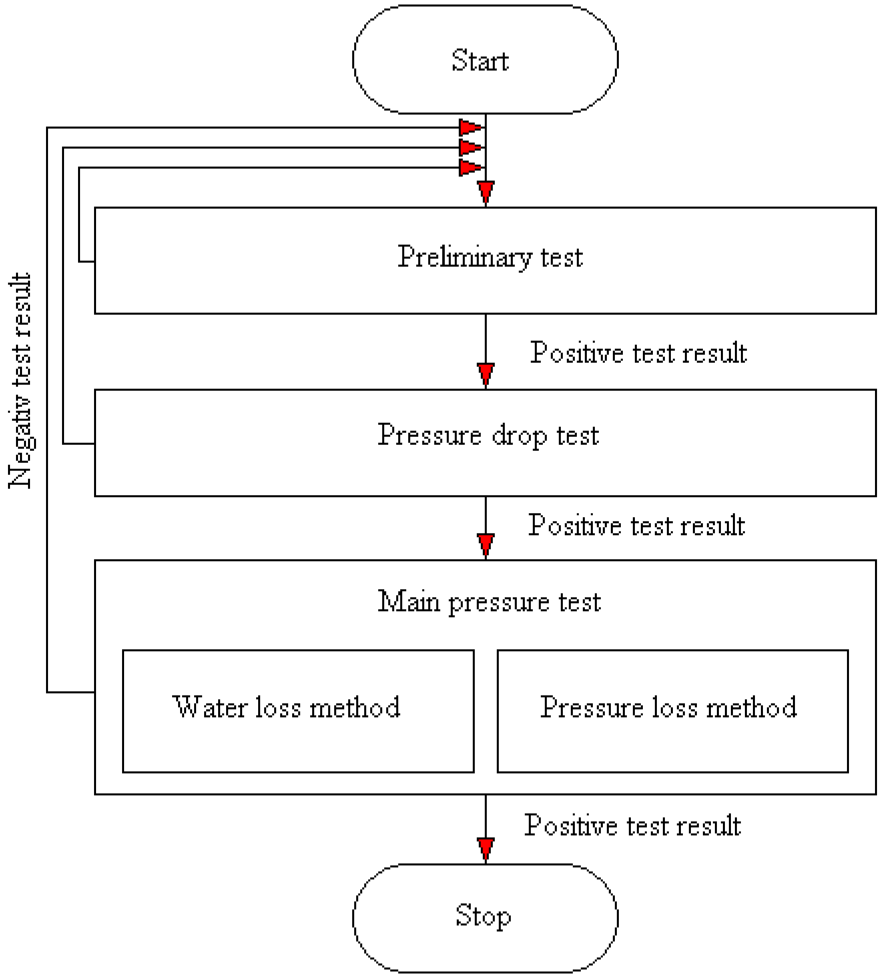

Figure 6. Test procedure for pipelines with viscoelastic properties

The duration of the preliminary test depends on the materials from which the pipeline is made and should be determined by the designer, taking into account the relevant product standards. The purpose of the preliminary test is to stabilize the pipeline position by achieving the most time-variable displacements. And prior to the main test, achieving the appropriate water saturation and achieving a pressure-dependent increase in the pipeline volume (flexible pipes). The main test phase may be repeated only after the entire test procedure (Fig. 6) has been repeated, including ensuring a relaxation time of not less than 60 minutes in the preliminary phase. After the relaxation period, quickly increase the pressure continuously, in less than 10 minutes, to the test pressure of the STP system (test pressure determined on the basis of 11.2.3 of the standard PN-EN 805: December 2002). Maintain the STP pressure for 30 minutes by pumping continuously or with short interruptions, and during this time carry out a control checking for any actual leaks. Then, stop pumping and observe for 1 hour the pressure changes caused by the elongation of the pipeline due to viscoelastic creep. Read the pressure value after this time has elapsed. If the preliminary phase is completed with a positive result, continue the testing procedure. An example of a pressure test for a pipeline with viscoelastic properties is shown in Figure 7.

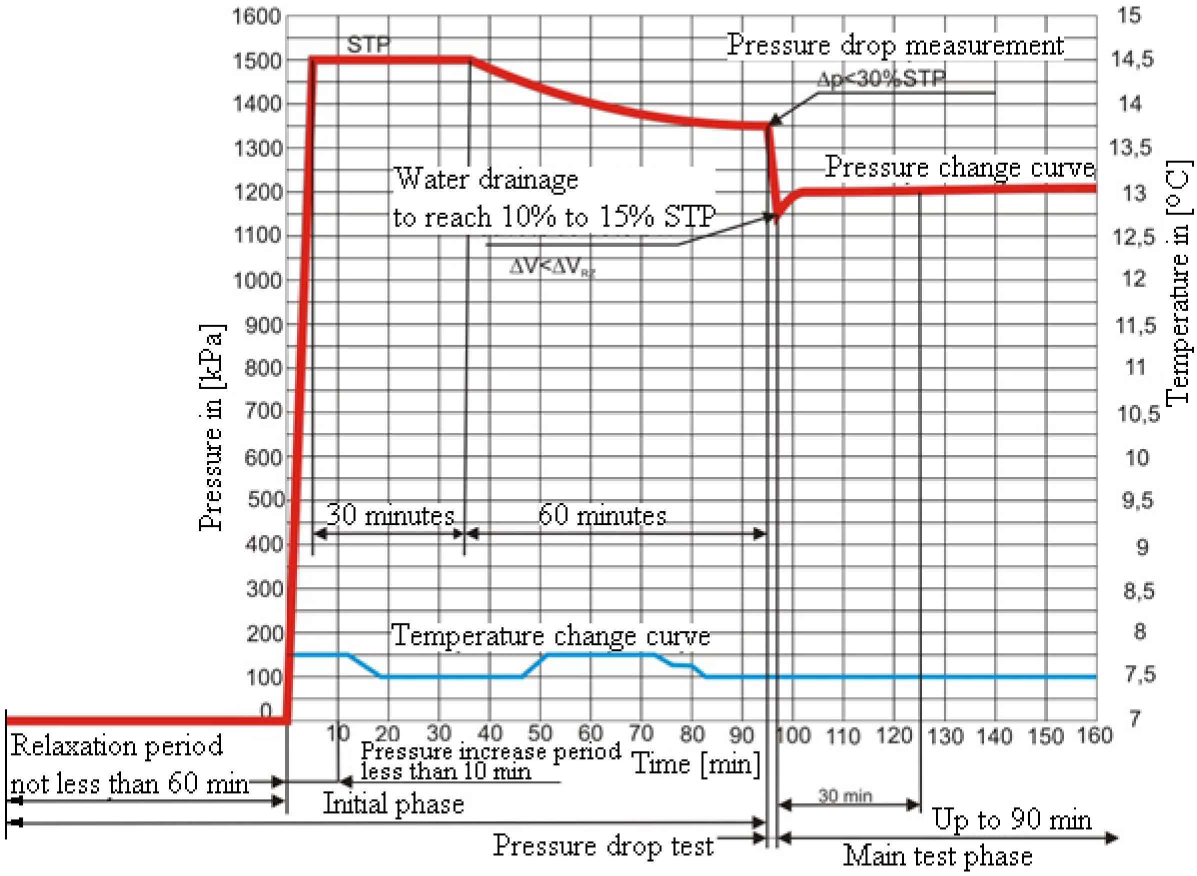

Figure 7. Example of a pressure test for a pipeline with viscoelastic properties

The integrated pressure drop test interrupts the viscoelastic creep caused by STP pressure-induced stresses. A sudden reduction in pressure leads to contraction of the pipeline. A correct evaluation of the basic leakproof test is possible provided that the air content inside the tested section is sufficiently low.

Therefore:

- when the preliminary phase ends it is necessary to rapidly reduce the pressure in the pipeline by Δp = 10÷15% STP by discharging water from the tested section;it is necessary to accurately measure the volume of discharged water ΔV;
- one should calculate the permissible water loss ΔV_{max} according to the equation (1) below and check that the amount of water released ΔV does not exceed the permissible value ΔV_{max}.

If ΔV is greater than ΔV_{max}, it means that the pipeline is air-filled, the test procedure should be interrupted, after depressurizing the tested pipeline (section) should be vented and the test should be repeated according to the algorithm presented in Figure 6.

$$\Delta V_{max} = 1{,}2 \cdot V \cdot \Delta p \left(\frac{1}{E_W} + \frac{D}{e \cdot E_R} \right) \tag{1}$$

where:

ΔV_{max} - permissible water loss in [litres]
V - volume of the tested pipeline section in [litres]
Δp - measured pressure drop in [kPa]
E_W - coefficient of water volume elasticity in [kPa] (2.1×10^6 kPa)
D - internal diameter of the pipe in [m]

e - pipeline wall thickness in [m]
E_R - modulus of elasticity in the circumferential direction depending on the pipe material in [kPa]
1,2 - correction factor (taking into account the air content) during the main pressure test.

If ΔV is less than ΔV_{max}, one should continue the test procedure while observing and recording - over a period of 30 minutes (main test phase, Fig. 7) - the pressure increase caused by pipeline shrinkage. The main test phase is considered successful (positive result) if the pressure curve shows a rising trend and this situation does not change in a 30-minute period which is usually long enough for the obtained results to be considered correct (reliable). If the obtained results raise doubts, then the main test phase should be extended to 90 minutes and the pressure drop should be limited to 25 kPa, counting from the maximum value that occurred in the contraction phase. If the pressure drop in this phase is greater than 25 kPa, the test has a negative result.

5. SUMMARY

Because of phenomena occurring during the action of pressure during a pressure test for flexible pipes made of viscoelastic materials, further application of the PN-B-10725 standard from 1997 referred to here is unjustified, as shown above. Currently, one can use the PN-EN 805 standard, and PN-C-89224 standard (which, however, does not have the status of a European standard) which refers to the PN-EN 805 standard in its scope and does not cause any functional conflict between the two standards.

Once again, the designer's role should be emphasized, especially when defining the detailed rules for the duration of the preliminary phase of the test, depending on the type of pipe material used.

Testing not in conformity with the requirements of the PN-EN 805 standard: December 2002, for modern plastic material solutions may lead to incorrect interpretation of the obtained test results which may lead to unjustified repetition of tests and unnecessary increase in costs during the investment implementation phase.

Literature:

1. Bolt A., Suligowski Z.; Próby szczelności rurociągów ciśnieniowych z tworzyw polimerowych. INSTAL 7-8/2007, str. 70.
2. Kuliczkowski A.; Rury kanalizacyjne, Własności materiałowe, Monografia, Wydawnictwo Politechniki Świętokrzyskiej, Kielce 2001 r.
3. Żuchowska D.; Polimery konstrukcyjne, WNT, Warszawa 2000 r. „Design of Buried Thermoplastics Pipes. Results of European Research Project". TEPPFA, March 1999.
4. Instalacje wodociągowe i kanalizacyjne, I Konferencja Naukowo Techniczna, Wydawnictwo Szeidel-Przywecki Sp. z o.o., 2004 r.
5. Polska Norma PN-EN 805: grudzień 2002, Zaopatrzenie w wodę. Wymagania dotyczące systemów zewnętrznych i ich części składowych, PKN, Warszawa 2002.
6. Polska Norma PN-ENV 1046: kwiecień 2007, Systemy przewodów rurowych z tworzyw sztucznych. Systemy poza konstrukcjami budynków do przesyłania wody lub ścieków. Praktyka instalowania pod ziemią i nad ziemią.
7. Polska Norma PN-B-10725: grudzień 1997, Wodociągi. Przewody zewnętrzne. Wymagania i badania. PKN, Warszawa 1997 r.
8. Polska Norma PN-C-89224:2018-03, Systemy przewodów rurowych z termoplastycznych tworzyw sztucznych. Zewnętrzne systemy bezciśnieniowe i ciśnieniowe do przesyłania wody, odwadniania i kanalizacji z nieplastyfikowanego poli(chlorku winylu) (PVC-U), polipropylenu (PP) i polietylenu (PE). Warunki techniczne wykonania i odbioru. PKN, 27.03.2018 r.
9. Poradnik „Tworzywa sztuczne", WNT, Warszawa 2000 r.

The relationship between the type of structure and the number of construction disasters

Jarosław Mikołajczyk

PhD., State University of Applied Sciences in Piła, Department of Mechanical Engineering, ul. Podchorążych 10, Piła, Poland, e-mail: jmikolajczyk@ans.pila.pl , ORCID: https://orcid.org/0000-0001-9196-0039

Abstract: This paper presents an analysis of the relationship between the type of construction and the number of construction disasters. One of the key elements which have an impact on the course and consequences of such events is the type of building structure. The type of applied construction determines how the building responds to various loads, including those caused by environmental factors, design and construction errors, as well as sudden and unforeseen events. Understanding how different types of structures affect building safety allows for better design and construction decisions which shall ultimately contribute to increasing the safety of people using these buildings and minimizing the risk of building disasters. In this paper, the following types of building structures were distinguished: brick, wooden, steel, prefabricated reinforced concrete, monolithic reinforced concrete and other (e.g. mixed). One can notice that, in quantitative terms, the biggest number of construction disasters in the discussed period concerned brick structures but only because their number is the greatest at present, and not because they are the most susceptible to disasters. The lowest number of construction disasters occurred in monolithic reinforced concrete structures because this type of structure is the smallest in number, it is the most expensive and has the highest strength coefficient. The calculated correlation value between the total number of construction disasters and the number of construction disasters of monolithic reinforced concrete structures practically proves the lack of relationship between the above mentioned variables. However, the calculated correlation value between the total number of construction disasters and the number of construction disasters of prefabricated reinforced concrete structures indicates a moderate correlation between the above mentioned variables and takes a negative value. However, there is a very high correlation between the total number of construction disasters and the number of construction disasters of mixed buildings (Pearson at the level of 0.80; Spearman at the level of 0.74), which means that these variables are dependent on each other. The highest correlation values were obtained for the number of disasters of brick objects and for wooden structures. The dependencies are practically functional, i.e. the number of construction disasters involving brick and wooden structures strongly depends on the total number of construction disasters.

Keywords: correlation, Pearson method, Spearman method, construction disasters

1. ANALYSIS OF CONSTRUCTION DISASTERS IN POLAND DEPENDING ON THE TYPE OF STRUCTURE

One of the key factors influencing the course and consequences of such events is the type of building structure. The type of applied construction determines how the building responds to various loads, including those caused by environmental factors, design and construction errors, as well as sudden and unforeseen events. Understanding how different types of structures affect building safety allows for better design and construction decisions which shall ultimately contribute to increasing the safety of people using these buildings and minimizing the risk of building disasters.

In this paper, the following types of building structures were distinguished:

- brick;
- timber;
- steel;
- prefabricated reinforced concrete;
- monolithic reinforced concrete;
- other (e.g. mixed).

Fig. 1 graphically presents the numbers of construction disasters in Poland in the years 2010÷2020 in chronological order. In the group of all these disasters we have disasters in brick, timber, steel, prefabricated reinforced concrete, monolithic reinforced concrete and other types of facilities (e.g. mixed). These numbers are different in different years. However, when we compare the numerical values of construction disasters in the appropriate order, certain relationship can be observed. Table 1 presents a a list of the total number of construction disasters in ascending order and the corresponding numbers of construction disasters in brick facilities. This is presented graphically in Fig. 2. One can see here an almost regular relationship between the increase in the number of construction disasters involving brick facilities and the increase in the total number of construction disasters. The only exceptions are two cases, two years, when this trend changed. This was the case in 2012 and 2011 when - while the total number of construction disasters increased - there was a decrease in the number of construction disasters involving brick facilities. This does not change the fact, however, that the number of construction disasters involving brick facilities is strongly dependent on the total number of construction disasters. Correlations between the above-mentioned variables were calculated in R [10, 11, 12] (Table 2). The following correlation values calculated using the Pearson's and Spearman's methods were obtained: 0.9485742 and 0.9636364, respectively. This result means that the correlation is so strong that it is actually functional. Based on actual statistical data, a first-order regression formula was determined for the number of construction disasters in brick facilities and, based on this formula, a mathematical model, the predicted numbers of construction disasters in brick facilities were determined (Table 3), which is shown in Fig. 3.

Fig. 1. The number of construction disasters in Poland in the years 2010-2020 in chronological order; x–axis – years; y-axis – number of disasters

Table 1. Summary of the total number of construction disasters in ascending order and the corresponding number of construction disasters in brick facilities

Total number of construction disasters	Number of construction disasters in brick facilities	Year
209	125	2014
249	143	2018
251	148	2019
258	155	2013
272	177	2020
307	179	2015
367	222	2016
426	209	2012
627	440	2017
648	360	2011
731	361	2010

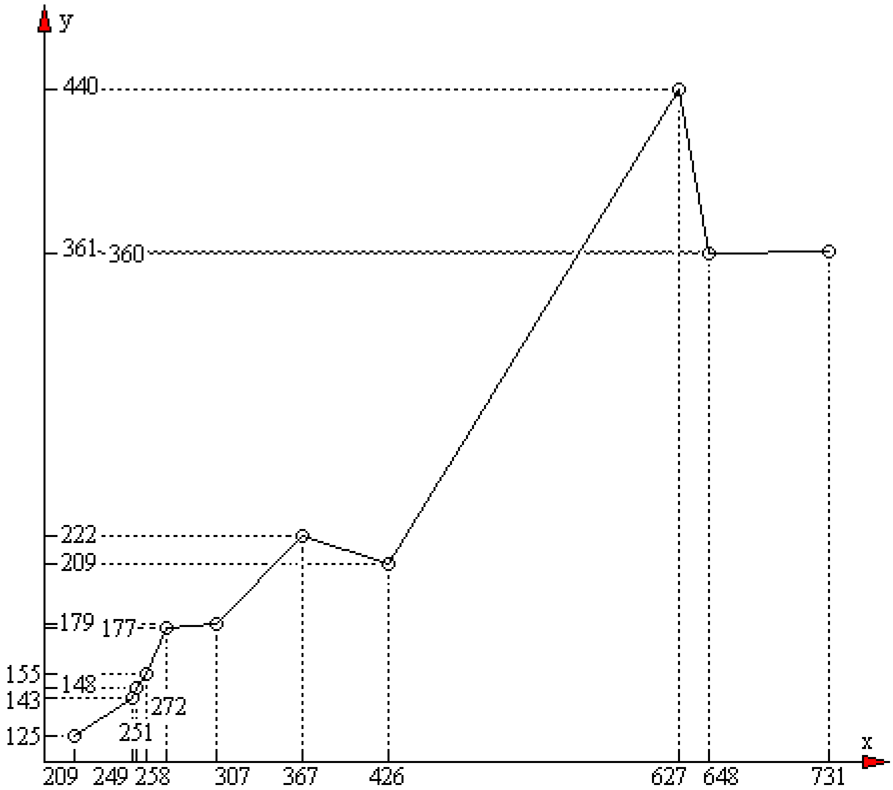

Fig. 2. Graphical presentation of the total number of construction disasters in Poland in the years 2010-2020 with the number of construction disasters in brick facilities; x-total number of construction disasters in Poland between 2010-2020; y-number of construction disasters in brick facilities

Table 2. Determining the correlation between the total number of construction disasters and the number of construction disasters in brick facilities in Poland between 2010-2020

Total number of construction disasters	Number of construction disasters in brick facilities	Pearson correlation	Spearman correlation
209	125	0.9485742	0.9636364
249	143		
251	148		
258	155		
272	177		
307	179		
367	222		
426	209		
627	440		
648	360		
731	361		

Based on statistical data and using R [13, 14, 15] software, the first-order regression formula for the number of construction disasters in brick facilities was determined:

$$y = 0{,}5432 \cdot x + 14{,}4518 \quad (1)$$

where:

x - total number of construction disasters in Poland in the years 2010-2020;

y - number of construction disasters in brick facilities

Of course, the above formula is only a mathematical model. Similar models can be specified for second, third, and higher order regressions.

Table 3. Summary of the total number of construction disasters in ascending order and corresponding numbers of construction disasters in brick facilities and the numbers of construction disasters in brick building calculated on the basis of the simple regression model

Total number of construction disasters in Poland in the years 2010-2020	Number of construction disasters in brick facilities	Number of construction disasters in brick facilities according to the first-order regression model	Number of construction disasters in brick facilities according to the first-order regression model after rounding to integers
209	**125**	127.98	**128**
249	**143**	149.71	**150**
251	**148**	150.79	**151**
258	**155**	154.59	**155**
272	**177**	162.20	**162**
307	**179**	181.21	**181**
367	**222**	213.80	**214**
426	**209**	245.85	**246**
627	**440**	355.04	**355**
648	**360**	366.45	**366**
731	**361**	411.53	**412**

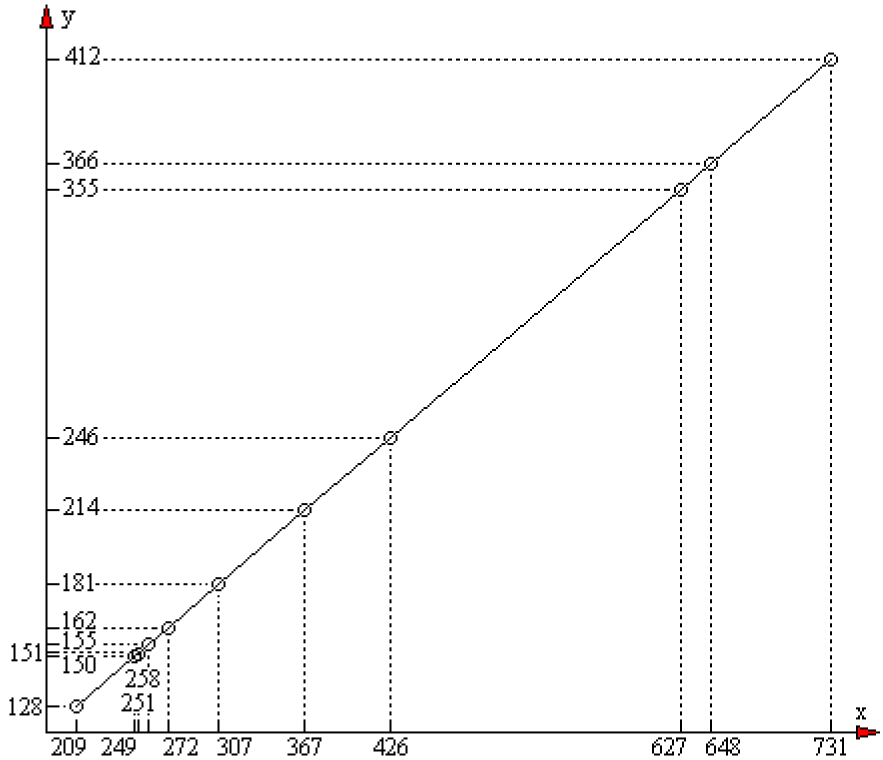

Fig. 3. Graphical presentation of the total number of construction disasters in Poland between 2010-2020 with the number of construction disasters in brick facilities calculated on the basis of the first-order regression mathematical model, rounded to integer numbers; x-total number of construction disasters in Poland between 2010-2020; y-number of construction disasters in brick buildings determined on the basis of a mathematical model

Table 4 presents a list of the total number of construction disasters in ascending order and the corresponding numbers of construction disasters in timber facilities. This is presented graphically in Fig. 4. One can notice here an almost regular relationship between the increase in the number of construction disasters involving timber facilities and the increase in the total number of construction disasters. The exceptions here are three cases, years 2010, 2017 and 2013, when this trend changed. In those years, the increase in the total number of construction disasters was accompanied by a decrease in the number of disasters involving timber structures. This does not change the fact that also in this case, as in the case of brick structures, there is a strong relationship between the number of construction disasters in timber facilities and the total number of construction disasters. The correlation value between the above-mentioned variables was calculated in R (Table 5). The following correlation values calculated using the Pearson's and Spearman's methods were obtained: 0.8853071 and 0.9090909, respectively. These results indicate that this correlation is so strong that it is actually a functional dependence. Based on actual statistical data, determined was a first-order regression formula for the number of construction disasters in timber structures.

Table 4. Summary of the total number of construction disasters in ascending order and the corresponding numbers of construction disasters in timber structures

Total number of construction disasters	y - number of construction disasters in timber structures	Year
209	26	2014
249	34	2018
251	38	2019
258	33	2013
272	45	2020
307	52	2015
367	81	2016
426	111	2012
627	103	2017
648	126	2011
731	101	2010

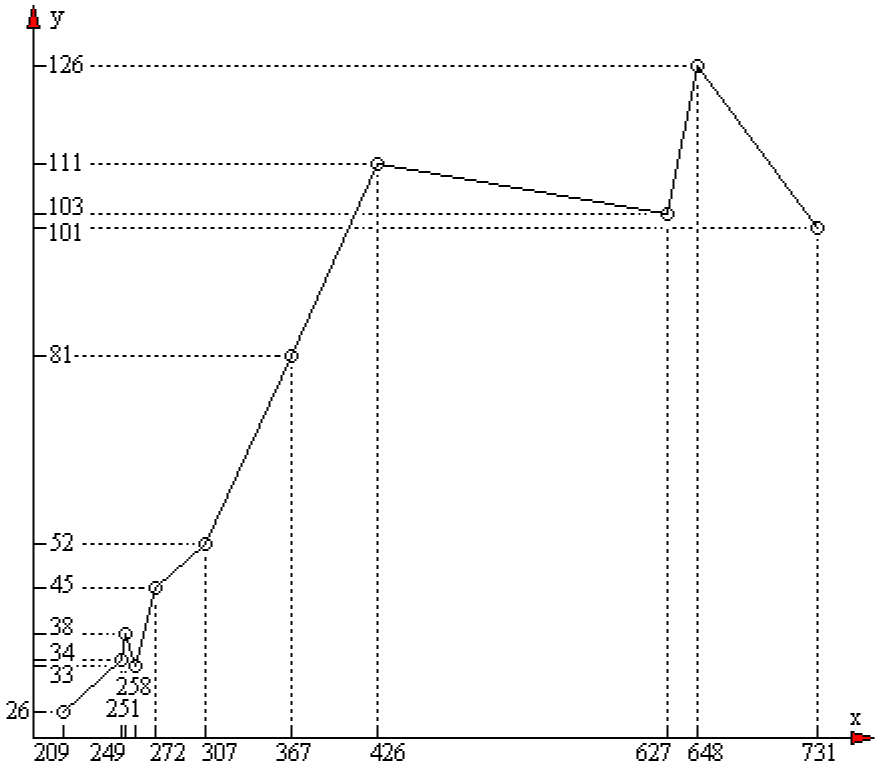

Fig. 4. Graphical presentation of the total number of construction disasters in Poland in the years 2010-2020 with the number of construction disasters in timber structures; x-total number of construction disasters in Poland between 2010-2020; y-number of construction disasters in timber structures

Table 5. Determining the correlation between the total number of construction disasters and the number of construction disasters in timber structures in Poland between 2010-2020

Total number of construction disasters	Number of construction disasters in brick facilities	Pearson correlation	Spearman correlation
209	26	0,8853071	0,9090909
249	34		
251	38		
258	33		
272	45		
307	52		
367	81		
426	111		
627	103		
648	126		
731	101		

Based on statistical data and using R, the first-order regression formula for the number of construction disasters in timber facilities was determined:

$$y = 0{,}1738 \cdot x - 0{,}4874 \quad (2)$$

where:

x - total number of construction disasters in Poland in the years 2010-2020;

y - number of construction disasters in timber structures

Of course, the above formula is only a mathematical model. The results must be rounded to integers.

Table 6 presents a list of the total number of construction disasters in ascending order and the corresponding numbers of construction disasters in mixed structures. This is presented graphically in Fig. 5. A significant irregularity between these variables can be noticed, i.e. when one variable increases, the other also increases, and then decreases. However, the calculated value of correlation between the above-mentioned variables (Table 7) indicates a relatively high correlation between them. The obtained values are at the level of 0.8022007 (correlation determined using the Pearson method) and 0.7443 (correlation determined using the Spearman method). This is not a functional dependence, but it is still large, which means that the above-mentioned variables are dependent on each other.

Table 6. A list of the total number of construction disasters in ascending order and the corresponding numbers of construction disasters in mixed structures

Total number of construction disasters	The number of construction disasters of mixed structures	Year
209	41	2014
249	57	2018
251	51	2019
258	50	2013
272	39	2020
307	57	2015
367	50	2016
426	89	2012
627	58	2017
648	135	2011
731	231	2010

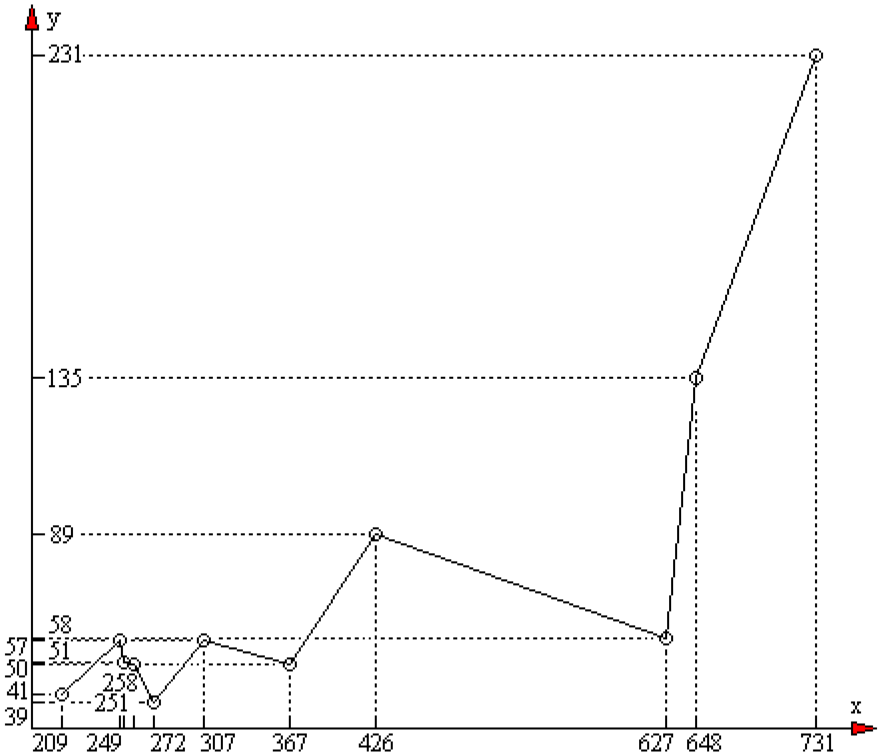

Fig. 5. Graphical presentation of the total number of construction disasters in Poland in the years 2010-2020 with the number of construction disasters in mixed structures; x-total number of construction disasters in Poland between 2010-2020; y-number of construction disasters of mixed structures

Table 7. Determining the correlation between the total number of construction disasters and the number of construction disasters in mixed structures in Poland in the years 2010-2020

Total number of construction disasters	The number of construction disasters in mixed structures	Pearson correlation	Spearman correlation
209	41	0.8022007	0.7443
249	57		
251	51		
258	50		
272	39		
307	57		

367	50		
426	89		
627	58		
648	135		
731	231		

Table 8 presents a summary of the total number of construction disasters in ascending order and the corresponding numbers of construction disasters in prefabricated reinforced concrete structures. This is presented graphically in Fig. 6. A significant irregularity between these variables can be noticed, i.e. when one variable increases, the other usually decreases. However, the calculated value of correlation between the above-mentioned variables (Table 9) indicates a moderately weak correlation between them. The obtained values are at the level of -0.553395 (correlation determined using the Pearson method) and -0.4567552 (correlation determined using the Spearman method). Both correlations are negative. This is obviously not a functional dependence, but it does exist, even though it is relatively weak, i.e. the above-mentioned variables are only partially dependent on each other.

Table 8. List of the total number of construction disasters in ascending order and the corresponding number of construction disasters in prefabricated reinforced concrete structures

Total number of construction disasters	Number of construction disasters in prefabricated reinforced concrete structures	Year
209	6	2014
249	3	2018
251	4	2019
258	5	2013
272	4	2020
307	6	2015
367	3	2016
426	4	2012
627	2	2017
648	4	2011
731	3	2010

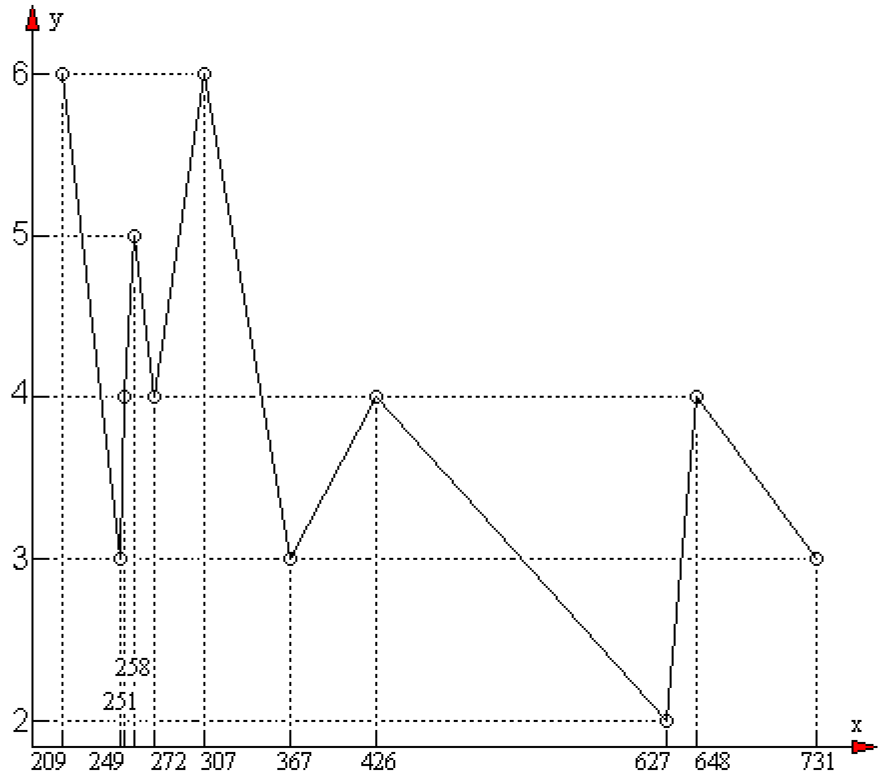

Fig. 6. Graphical presentation of the total number of construction disasters in Poland in the years 2010-2020 with the number of construction disasters in prefabricated reinforced concrete structures; x-total number of construction disasters in Poland between 2010-2020; y-number of construction disasters in prefabricated reinforced concrete structures

Table 9. Determining the correlation between the total number of construction disasters and the number of construction disasters in prefabricated reinforced concrete structures in Poland between 2010-2020

Total number of construction disasters	Number of construction disasters in prefabricated reinforced concrete structures	Pearson correlation	Spearman correlation
209	6	- 0,553395	- 0,4567552
249	3		
251	4		
258	5		
272	4		
307	6		
367	3		
426	4		
627	2		
648	4		
731	3		

Table 10 presents a summary of the total number of construction disasters in ascending order and the corresponding numbers of construction disasters in monolithic reinforced concrete structures. This is presented graphically in Fig. 7. There is considerable irregularity between these variables. The calculated value of correlation between the above-mentioned variables (Table 11) proves that there is practically no dependence between them. The obtained values are at the level of 0.4388822 (correlation determined using the Pearson method) and 0.2286323 (correlation determined using the Spearman method).

Table 10. Summary of the total number of construction disasters in ascending order and the corresponding numbers of construction disasters in monolithic reinforced concrete structures

Total number of construction disasters	Number of construction disasters in monolithic reinforced concrete structures	Year
209	4	2014
249	1	2018
251	1	2019
258	4	2013
272	1	2020
307	1	2015
367	1	2016
426	1	2012
627	3	2017
648	2	2011
731	6	2010

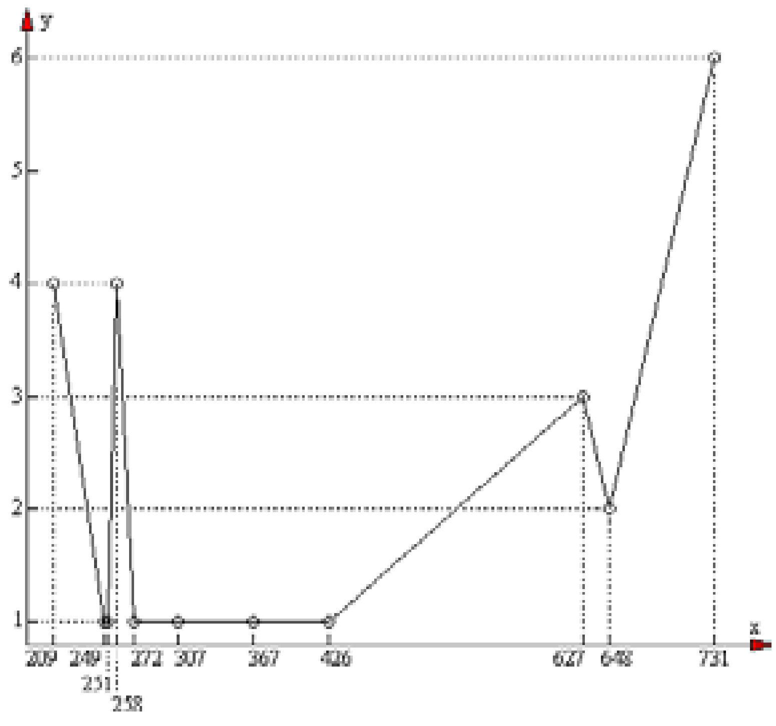

Fig. 7. Graphical presentation of the total number of construction disasters in Poland in the years 2010-2020 with the number of construction disasters in monolithic reinforced concrete structures; x-total number of construction disasters in Poland between 2010-2020; y-number of construction disasters in monolithic reinforced concrete structures

Table 11. Determining the correlation between the total number of construction disasters and the number of construction disasters in monolithic reinforced concrete structures in Poland between 2010-2020

Total number of construction disasters	Number of construction disasters in monolithic reinforced concrete structures	Pearson correlation	Spearman correlation
209	4	0.4388822	0.2286323
249	1		
251	1		
258	4		
272	1		
307	1		
367	1		
426	1		
627	3		
648	2		
731	6		

References

[1] J. Koronacki, J. Mielniczuk: "Statystyka dla studentów kierunków technicznych i przyrodniczych". Wydawnictwo WNT, Warszawa, 2018.
[2] M. Krzysztofiak, D. Urbanek: „Metody statystyczne". Państwowe Wydawnictwo naukowe, Warszawa, 1977.
[3] M. Krzyśko: „Statystyka matematyczna". Wydawnictwo Naukowe Uniwersytetu Adama Mickiewicza w Poznaniu, Poznań, 1996.
[4] A. Luszniewicz: „Statystyka ogólna". Państwowe Wydawnictwo Ekonomiczne, Warszawa, 1987.
[5] W. Żakowski, W. Kołodziej: „Matematyka cz. II. Analiza matematyczna". Wydawnictwo Naukowo-Techniczne, Warszawa, 2003.
[6] Główny Urząd Nadzoru Budowlanego – Katastrofy budowlane w latach 2004-2022, Warszawa, 2005-2023
[7] P. Biecek: „Przewodnik po pakiecie R". Oficyna Wydawnicza GIS, Wrocław, 20017.
[8] P. Biecek: „Analiza danych z programem R. Modele liniowe z efektami stałymi, losowymi i mieszanymi". Wydawnictwo Naukowe PWN, Warszawa, 2013.
[9] M. Crawley: „The R Book". Willey-Blackwell, 2012.
[10] B. Everitt, T. Hothorn: „A Handbook of Statistical Analyses Using R". Chapman&Hall/CRC Computer Science & Data Analyses, 2010.
[11] M. Gągolewski: „Programowanie w języku R. Analiza danych, obliczenia, symulacje". Wydawnictwo Naukowe PWN S.A., Warszawa, 2016.
[12] C. Gillespie, R. Lovelace: „Wydajne programowanie w R. Praktyczny przewodnik po lepszym programowaniu". APN Promise, Warszawa, 2018.

Zależność między rodzajem konstrukcji, a liczbą katastrof budowlanych

Słowa kluczowe: korelacja, metoda Pearson'a, metoda Spearman'a, katastrofy budowlane

STRESZCZENIE: W pracy przedstawiono określenie zależności między rodzajem konstrukcji, a liczbą katastrof budowlanych. Jednym z kluczowych czynników wpływających na przebieg i skutki takich zdarzeń jak katastrofy budowlane jest rodzaj konstrukcji budynku. Rodzaj zastosowanej konstrukcji determinuje, w jaki sposób budynek reaguje na różnorodne obciążenia, w tym spowodowane czynnikami środowiskowymi, błędami projektowymi, wykonawczymi, a także nagłymi i nieprzewidzianymi zdarzeniami. Zrozumienie, jak różne typy konstrukcji wpływają na bezpieczeństwo budynków, pozwala na podejmowanie lepszych decyzji projektowych i

konstrukcyjnych, co w efekcie przyczynia się do zwiększenia bezpieczeństwa użytkowników budynków oraz minimalizacji ryzyka katastrof budowlanych. W niniejszej pracy wyróżniono następujące rodzaje konstrukcji budowlanych: murowane, drewniane, stalowe, żelbetowe prefabrykowane, żelbetowe monolityczne, inne (np. mieszane). W pracy zauważono, że pod względem ilościowym najwięcej katastrof budowlanych w omawianym okresie czasu dotyczyło obiektów murowanych, ale tylko dlatego, że obecnie jest ich najwięcej, a nie dlatego, że są najbardziej podatne na katastrofy. Najmniej katastrof budowlanych dotyczyło konstrukcji żelbetowych monolitycznych, ponieważ jest ich ilościowo najmniej, są najbardziej kosztowne oraz mają najwyższy współczynnik wytrzymałości. Obliczona wartość korelacji pomiędzy całkowita liczbą katastrof budowlanych, a liczbą katastrof budowlanych obiektów żelbetowych monolitycznych świadczy praktycznie o braku zależności między w/w zmiennymi. Natomiast obliczona wartość korelacji pomiędzy całkowita liczbą katastrof budowlanych, a liczbą katastrof budowlanych obiektów żelbetowych prefabrykowanych świadczy o umiarkowanej korelacji między w/w zmiennymi i przyjmuje wartość ujemną. Natomiast występuje bardzo duża wartość korelacji między całkowitą liczba katastrof budowlanych, a liczba katastrof budowlanych obiektów mieszanych (Pearson na poziomie 0,8; Spearman na poziomie 0,74), czyli te zmienne są od siebie zależne. Największe wartości korelacji otrzymano dla katastrof obiektów murowanych oraz dla obiektów drewnianych. Zależności są wręcz funkcyjne, czyli liczby katastrof obiektów murowanych i obiektów drewnianych silnie zależą od całkowitej liczby katastrof budowlanych.

The correlation between the population and number of construction disasters

Jarosław Mikołajczyk

PhD., State University of Applied Sciences in Piła, Department of Mechanical Engineering, ul. Podchorążych 10, Piła, Poland, e-mail: jmikolajczyk@ans.pila.pl , ORCID: https://orcid.org/0000-0001-9196-0039

1. Statistical analysis

Based on data contained in the General Office of Building Supervision in Poland and the Polish Central Statistical Office, the number of construction disasters was compared with the number of population of Poland at a given time. Then, correlations between the above-mentioned variables were calculated in R [10, 11, 12, 13, 14, 15]. Data and calculation results are included in Table 1.

Table 1. Comparison of the number of construction disasters with the number of population of Poland at a given time

Year	Number of disasters in Poland	Population of Poland [thousand]	Pearson correlation	Spearman correlation
2004	187	38174	- 0.1132023	- 0.03157895
2005	132	38157		
2006	338	38125		
2007	520	38116		
2008	1113	38136		
2009	264	38167		
2010	731	38530		
2011	648	38538		
2012	426	38533		
2013	258	38496		
2014	209	38479		
2015	307	38437		
2016	367	38433		
2017	627	38434		
2018	249	38411		
2019	251	38383		
2020	272	38089		
2021	469	37908		
2022	663	37766		

The correlation value between the number of disasters in Poland and the population of the entire country, calculated using the Pearson method, is very small, i.e. there is practically no relationship between these variables. The correlation calculated using Sperman's method also confirms this. The minus sign means that when one variable value increases, the other decreases and vice versa. Indeed, looking at graphical courses of the above-mentioned variables (Fig. 1 and Fig. 2) it is difficult to find any relationship between them. The above correlation result also proves that both variables (country population and number of disasters) are independent of each other.

The question arises here: is there any relationship between the number of disasters and the population of Poland in relation to a voivodeship, i.e. division into administrative regions? Table 2 presents a summary of the number of construction disasters for individual Polish voivodeships. On this basis, the correlation values between individual variables were recalculated in R. And Fig. 3 graphically presents the values of the numbers of construction disasters in Poland in the years 2010÷2020 for individual voivodeships. There is a very big range in numbers, from 47 disasters for the Warmińsko-Mazurskie Voivodeship to as many as 686 disasters for the Mazowieckie Voivodeship, i.e. over 14 times more. A terrifying value.

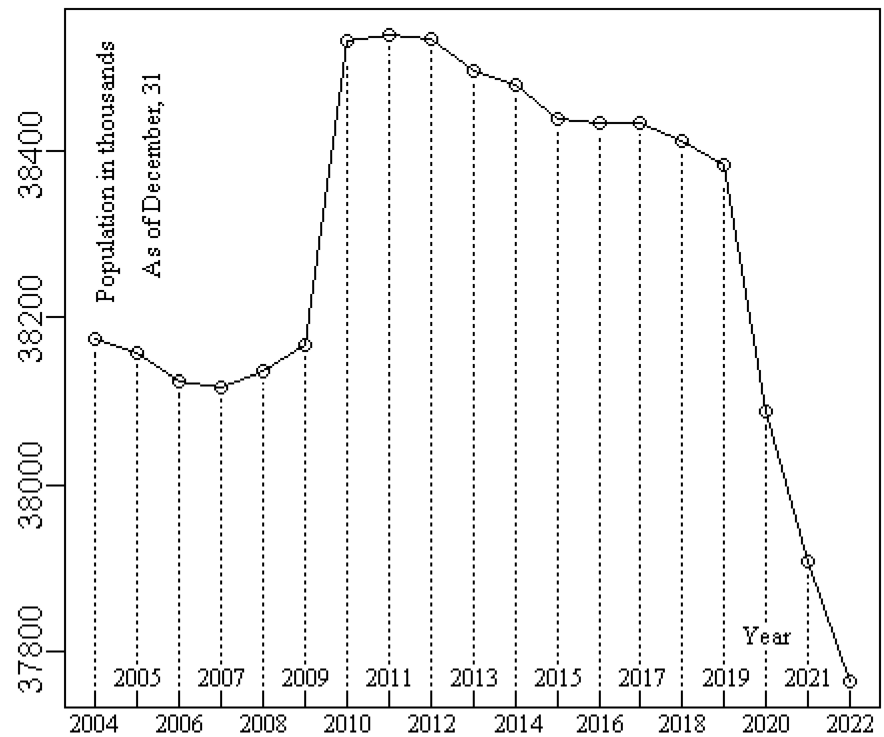

Fig. 1. Changes in the population of Poland in particular years

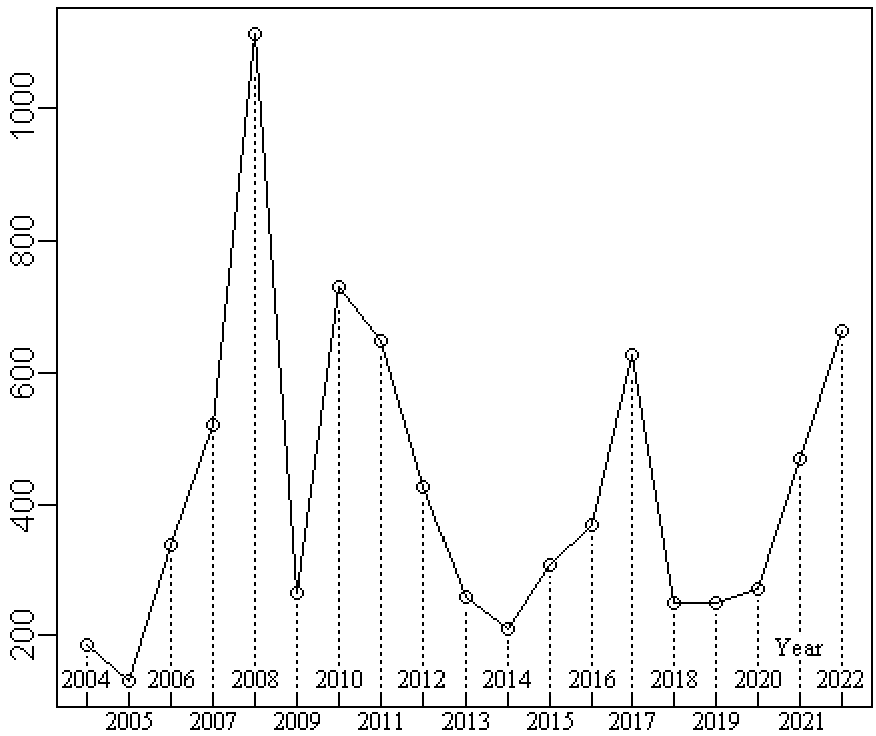

Fig. 2. Number of disasters in Poland in particular years

Table 2. 2 A list of number of construction disasters for individual Polish voivodeships

Voivodeship	Number of construction disasters in 2010-2020	Population of a given voivodeship in 2020 [thousand]	Pearson correlation	Spearman correlation
Warmińsko-Mazurskie	47	1416,5	0.6013826	0.4588235
Zachodnio-Pomorskie	60	1688,0		
Podkarpackie	88	2121,2		
Lubuskie	140	1007,1		
Dolnośląskie	147	2891,3		
Świętokrzyskie	183	1224,6		
Pomorskie	197	2346,7		
Śląskie	198	4492,3		
Kujawsko-Pomorskie	258	2061,9		
Opolskie	274	976,8		
Podlaskie	283	1173,3		
Małopolskie	353	3410,4		
Lubelskie	399	2095,3		
Łódzkie	468	2438,0		
Wielkopolskie	581	3496,5		
Mazowieckie	686	5425,0		

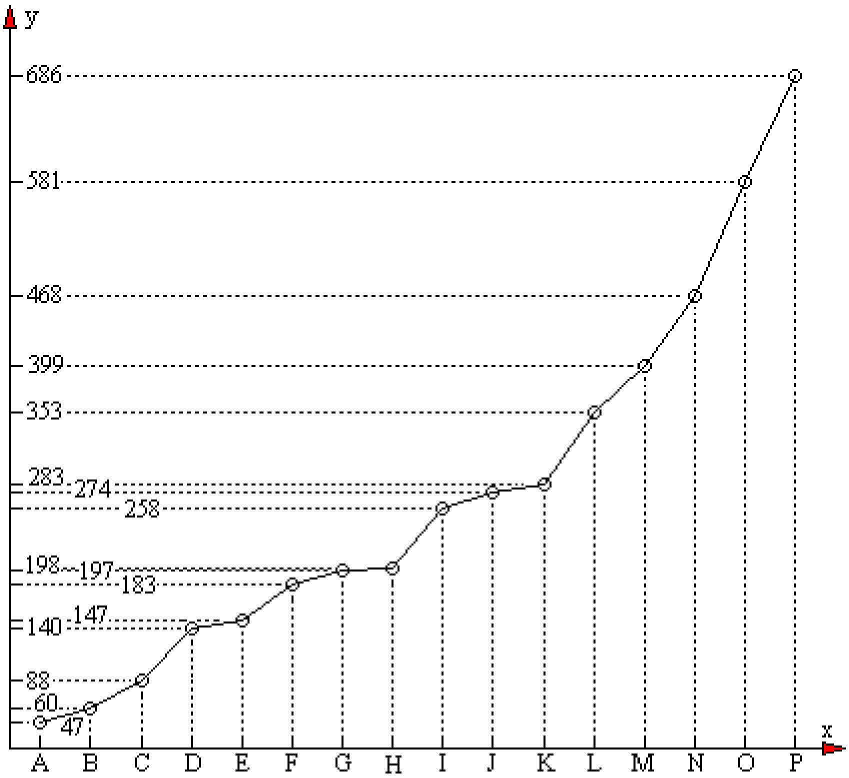

Fig. 3. A graphical presentation of the numbers of construction disasters in Poland in years 2010÷2020 for individual voivodeships.

x-axis – individual voivodeships; y-axis – number of construction disasters; A – Warmińsko-Mazurskie Voivodeship; B – Zachodnio-Pomorskie Voivodeship; C – Podkarpackie Voivodeship; D – LubuskieVoivodeship; E – Dolnośląskie Voivodeship; F – Świętokrzyskie Voivodeship; G – Pomorskie Voivodeship; H – Śląskie Voivodeship; I – Kujawsko-Pomorskie Voivodeship; J – Opolskie Voivodeship; K – Podlaskie Voivodeship; L – Małopolskie Voivodeship; M – Lubelskie Voivodeship; N – Łódzkie Voivodeship; O – Wielkopolskie Voivodeship; P – Mazowieckie Voivodeship

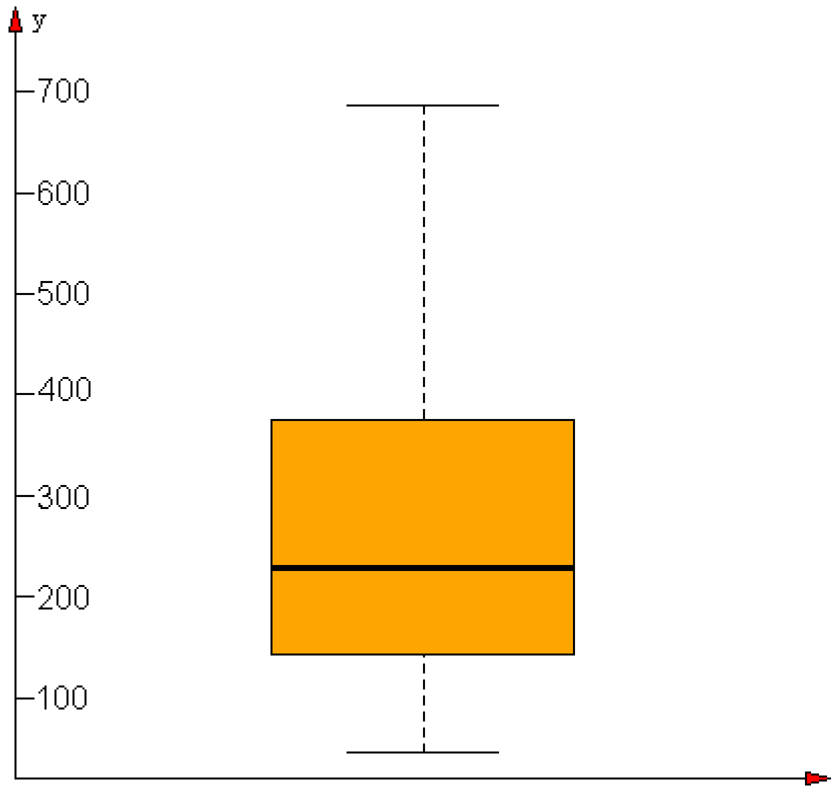

Fig. 4. A box plot generated in R showing the number of disasters for each voivodeship
y – number of disasters

Table 3. Summary of selected statistical parameters for the number of disasters in individual Polish voivodeships

Min.	1st Qu.	Median	3rd Qu.	Max.	IQR	R	s	d_1	Mean
47	145.2	228.0	364.5	686	219.25	639	184.3536	141.9531	272.6

- Min – minimum value;
- 1st Qu. – lower (first) sample quartile (Q_1);
- Median – median (‘median value’ Q_2);
- Mean – arithmetic mean;
- 3rd Qu. – upper (third) sample quartile (Q_3);
- Max. – maximum value;
- IQR – interquartile range;
- R – sample range;
- s – standard deviation;
- d_1 – average deviation from the mean value.

Of course (Fig. 4) the minimum value is in the Warmińsko-Mazurskie Voivodeship – 47 disasters (the lower “whisker of the graph”), the maximum value is in the Mazowieckie Voivodeship – 686 construction disasters (the upper “whisker of the graph”). Sample range (R) – this is the difference between the maximum value and the minimum value, i.e. 686 minus 47, i.e. 639 (the difference between the upper and lower “whiskers” of the graph) – Table 3. The standard deviation value is s=184.3536. The first quartile (lower part of the box) has the value 1stQu.=145.2. The third quartile (upper part of the box) has the value

3rdQu.=364.5. The median value is Median=228 construction disasters. The sample range R is very large. The mean value is unevenly distributed in the box plot. Whiskers very far from box plot. No outliers. Interquartile range IQR =219.25.

An interesting graph (Fig. 5) is for the density distribution of disaster values for individual voivodeships. The highest density of results is visible around the value of approximately 200 building disasters. And indeed, as many as three voivodeships have disaster numbers very close to this value. These include: Świętokrzyskie Voivodeship (183 disasters), Pomorskie Voivodeship (197 construction disasters) and Śląskie Voivodeship (198 construction disasters). N – means the number of measurements (in our case it is the number of voivodeships). Horizontal axis – the number of disasters. Of course, in our case the density is limited from the construction disaster value of 47 (Warmińsko-Mazurskie Voivodeship) to the value of 686 (Mazowieckie Voivodeship). Of course, there are no negative values for our case. A graph (Fig. 5) was built for values from minus 200 disasters (unrealistic value) to a value of 1000 disasters. The above graph would need to be cut in our case from value 47 to value 686. The density graph of construction disasters for individual Polish voivodeships is asymmetrically distributed (this is confirmed by the box plot – Fig. 4).

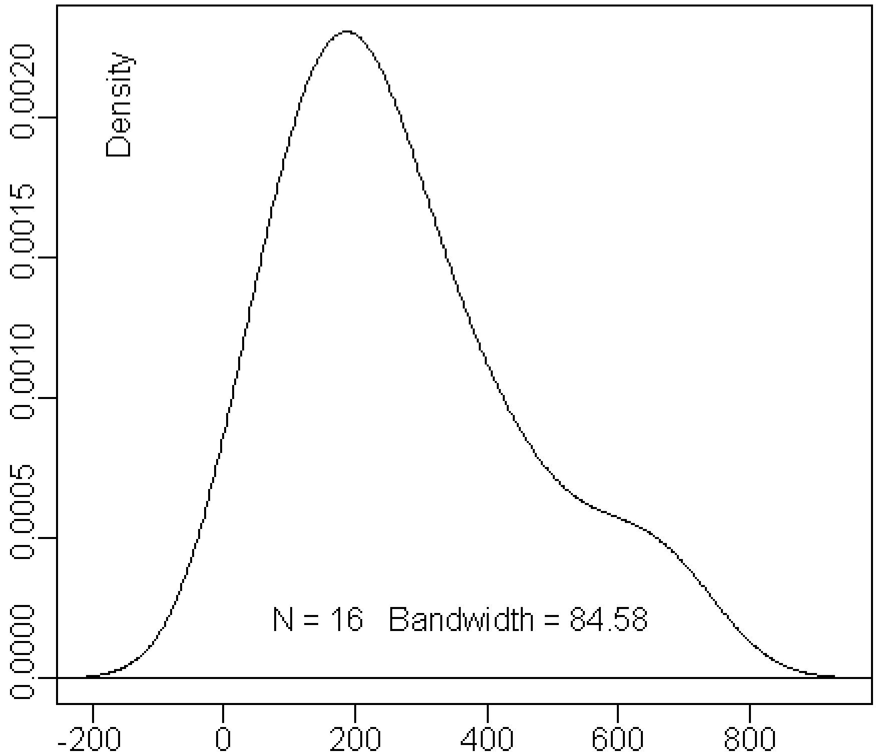

Fig. 5. Density distribution of disaster values for individual voivodeships

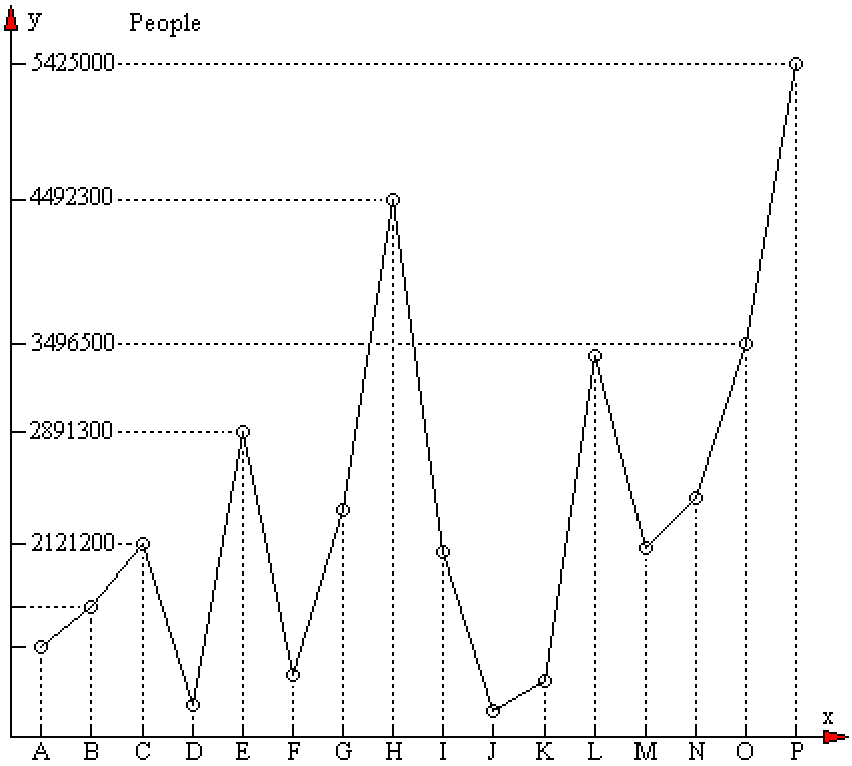

Fig. 6. Population in individual voivodeships in 2020 (same order as in Fig. 3, i.e. according to the increasing number of construction disasters)
x-axis – individual voivodeships; y-axis – number of construction disasters; A – Warmińsko-Mazurskie Voivodeship; B – Zachodnio-Pomorskie Voivodeship; C – Podkarpackie Voivodeship; D – LubuskieVoivodeship; E – Dolnośląskie Voivodeship; F – Świętokrzyskie Voivodeship; G – Pomorskie Voivodeship; H – Śląskie Voivodeship; I – Kujawsko-Pomorskie Voivodeship; J – Opolskie Voivodeship;K – Podlaskie Voivodeship; L – Małopolskie Voivodeship; M – Lubelskie Voivodeship; N – Łódzkie Voivodeship; O – Wielkopolskie Voivodeship;P – Mazowieckie Voivodeship

Looking at the graph in Fig. 3 and in Fig. 6, certain similarities can be observed, i.e. for increasing values of construction disasters we have partially increasing values of the population of a given voivodeship. This is the case, for example, of the last four voivodeships: Lubelskie (letter M), Łódzkie (letter N), Wielkopolskie (letter O) and Mazowieckie (letter P). The similarity is only partial, therefore the correlation is at the level of 0.6013826 (Pearson) and 0.4588235 (Spearman), i.e. moderate. That is why we see cases here, e.g. Opolskie voivodeship (letter J) which has a relatively large number of construction disasters (274 disasters) and the smallest population (976,800 people), i.e. it breaks away from this relationship. The situation is similar with Lubuskie voivodeship (letter D).

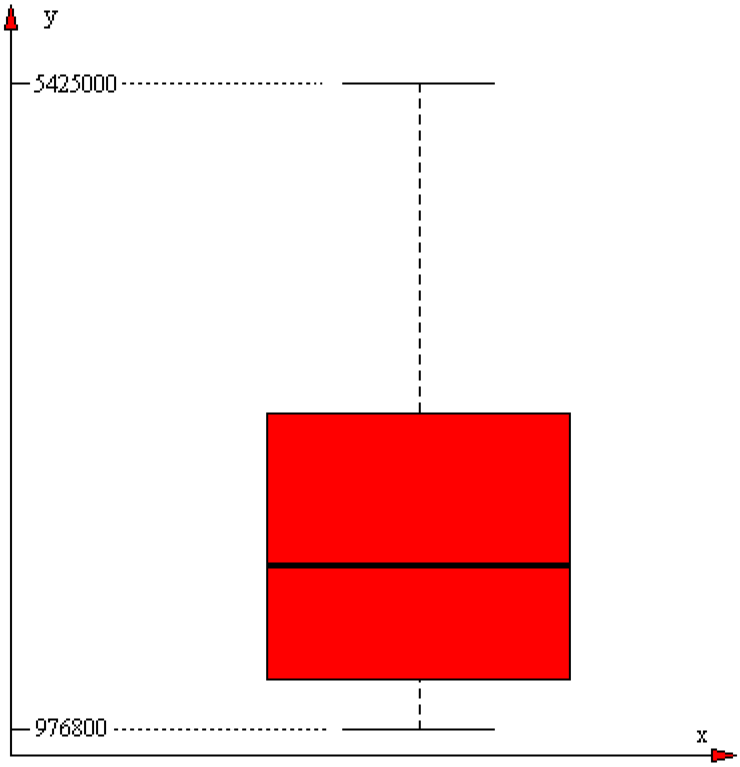

Fig. 7. Box plot generated in R showing the population numbers for individual voivodeships (the individual values of this plot are presented in Table 3)
y – number of people

Table 4. Selected statistical parameters for the number of people in individual Polish voivodeships

Min.	1st Qu.	Median	3rd Qu.	Max.	IQR	R	s	d_1	Mean
976800	1368525	2108250	3021075	5425000	1652550	4448200	1280813	975520,3	2391556

- Min – minimum value;
- 1st Qu. – lower (first) sample quartile (Q_1);
- Median – median (‘median value’ Q_2);
- Mean – arithmetic mean;
- 3rd Qu. – upper (third) sample quartile (Q_3);
- Max. – maximum value;
- IQR – interquartile range;
- R – sample range;
- s – standard deviation;
- d_1 – average deviation from the mean value.

Of course, in this comparison, Opolskie voivodeship has the lowest value (Min. parameter), and Mazowieckie voivodeship has the highest value (Max. parameter).

Fig. 8 presents the division of Poland into voivodeships. It can be noticed that the voivodeships with the highest number of disasters (Mazowieckie voivodeship) and the lowest number of disasters (Warmińsko-Mazurskie voivodeship) are adjacent to each other. It's hard to explain.

Fig. 8. Division of Poland by voivodeships (presented in ascending order by the number of construction disasters from the lowest value to the highest)
1 – Warmińsko-Mazurskie; 2- Zachodnio-Pomorskie; 3- Podkarpackie; 4 – Lubuskie; 5- Dolnośląskie; 6 – Świętokrzyskie; 7- Pomorskie; 8 – Śląskie; 9 – Kujawsko-Pomorskie; 10- Opolskie; 11 – Podlaskie; 12 – Małopolskie; 13 – Lubelskie; 14 – Łódzkie; 15 – Wielkopolskie; 16 – Mazowieckie

The last question which should be asked is this: is there a relationship (and what is its magnitude) between the population density of a given voivodeship (region) and the number of construction disasters in that region? Table 5 presents a comparison of the number of disasters with the population density for a given province, and the correlation between the above-mentioned variables was calculated using the Pearson and Spearman methods. The correlation values are 0.1710153 and 0.3080332, respectively. So the correlation is weak between them. Analysing data in Table 5 one can indeed see that the highest population density is in Małopolskie voivodeship (131 people/km^2) and Śląskie voivodeship (124 people/km^2). However, their places in terms of the number of construction disasters are quite distant - Małopolskie Voivodeship is on the 5th place, while Śląskie Voivodeship is on the 9th place, with Mazowieckie Voivodeship on the 1st place in terms of the number of construction disasters (i.e. the worst, most dangerous). Why is this so? It so probably because the place of residence is often not the same as the place of work. Construction disasters most often occur in workplaces because the structures in question are then more exposed to all kinds of vibrations, traffic accidents, etc. related to the movement of large quantities of cargo and people. Workplaces (shopping centres, factories, industrial centers) are often also military and terrorist targets. Home, on the other hand, is associated more with peace and relaxation.

An interesting case is Podkarpackie Voivodeship (Fig. 9) which has as many as 75 people/km^2 (which is almost 50% more than Mazowieckie Voivodeship with Warsaw!), but only 88 construction disasters in years 2010÷2020. In terms of safety, it is second only to Warmińsko-Mazurskie Voivodeship and Zachodniopomorskie Voivodeship. Thus, it is possible to have a big population density and a very small number of construction disasters. It is possible that the reason for this status is that authorities of this region are very particulate about such events.

Table 5. Comparison of the number of construction disasters for individual Polish voivodeships with population density

Voivodeship	Number of construction disasters in 2010-2020	Population density [person/km^2] in 2020	Pearson correlation	Spearman correlation
Warmińsko-Mazurskie	47	25	0.1710153	0.3080332
Zachodnio-Pomorskie	60	25		
Podkarpackie	88	75		
Lubuskie	140	27		
Dolnośląskie	147	52		
Świętokrzyskie	183	61		
Pomorskie	197	50		
Śląskie	198	124		
Kujawsko-Pomorskie	258	50		
Opolskie	274	54		
Podlaskie	283	24		
Małopolskie	353	131		
Lubelskie	399	47		
Łódzkie	468	54		
Wielkopolskie	581	57		
Mazowieckie	686	58		

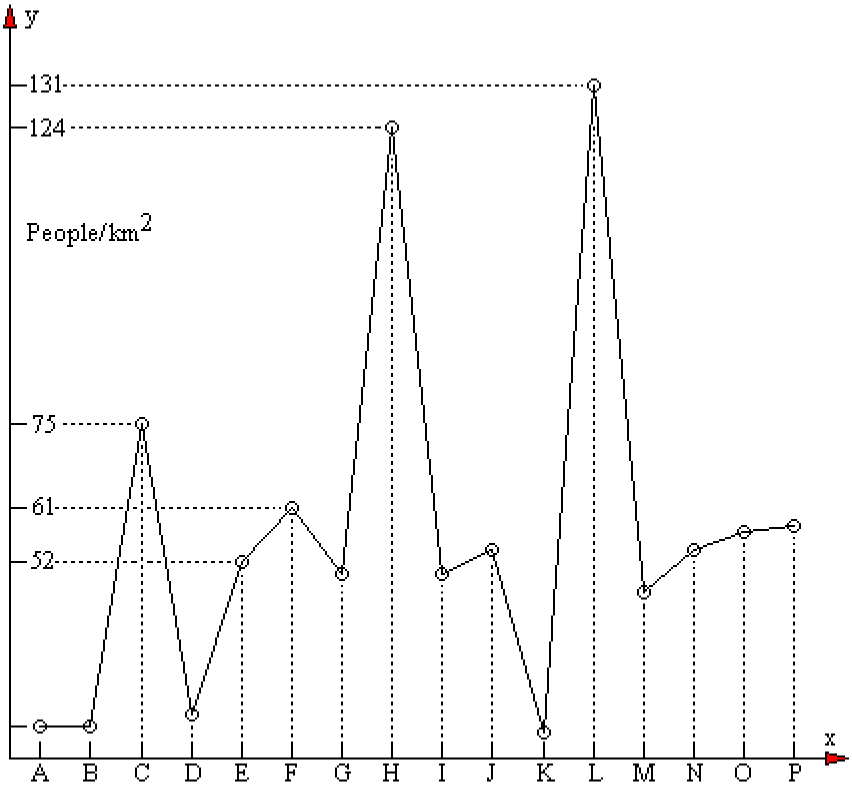

Fig. 9. Population density in individual voivodeships in 2020 (same order as in Fig. 3, i.e. according to the increasing number of construction disasters)
x-axis – individual voivodeships; y-axis – population density of a given voivodeship [person/km^2]; A – Warmińsko-Mazurskie Voivodeship; B – Zachodnio-Pomorskie Voivodeship; C – Podkarpackie Voivodeship; D – LubuskieVoivodeship; E – Dolnośląskie Voivodeship; F – Świętokrzyskie Voivodeship; G – Pomorskie Voivodeship; H – Śląskie Voivodeship; I – Kujawsko-Pomorskie Voivodeship; J – Opolskie Voivodeship;K – Podlaskie Voivodeship; L – Małopolskie Voivodeship; M – Lubelskie Voivodeship; N – Łódzkie Voivodeship; O – Wielkopolskie Voivodeship;P – Mazowieckie Voivodeship

3. Conclusion

Based on the above mathematical calculations, the following conclusion can be drawn.

The number of construction disasters in the country (Poland) and the population of Poland are independent of each other. This also means that the number of the country's population is decisively influenced by factors other than construction (of any type - whether land or sea, etc.). It is difficult to comment on the population number but we can guess that, for example, pandemics, disasters, agricultural disasters, droughts, the level of the economy, recession or wars may have a greater significance and a greater impact. This means that globally (with respect to the country), these variables (the country's population and the number of disasters in the country) are not dependent on each other.

However, locally, i.e. in relation to the region (in our case, the voivodeship), the number of disasters depends to some extent on the population of a given area. This is demonstrated by the correlation values calculated using the Pearson method (0.6013826) and the Spearman method (0.4588235). These are not functional dependencies, i.e. strong, but moderate dependencies. Therefore, one can say that the above-mentioned local variables (in relation to the region) are partially and moderately dependent on each other.

A mathematically defined relationship between the population density of a given voivodeship and the number of construction disasters occurring within its area is weak. This means that the above-mentioned variables are partly dependent on each other, but only slightly.

Similar results are expected for other countries and their regions/states/ counties/ provinces/districts/lands. Further studies will be continued in this direction.

References

[1] J. Koronacki, J. Mielniczuk: "Statystyka dla studentów kierunków technicznych i przyrodniczych". Wydawnictwo WNT, Warszawa, 2018.
[2] M. Krzysztofiak, D. Urbanek: „Metody statystyczne". Państwowe Wydawnictwo naukowe, Warszawa, 1977.
[3] M. Krzyśko: „Statystyka matematyczna". Wydawnictwo Naukowe Uniwersytetu Adama Mickiewicza w Poznaniu, Poznań, 1996.
[4] A. Luszniewicz: „Statystyka ogólna". Państwowe Wydawnictwo Ekonomiczne, Warszawa, 1987.
[5] W. Żakowski, W. Kołodziej: „Matematyka cz. II. Analiza matematyczna". Wydawnictwo Naukowo-Techniczne, Warszawa, 2003.
[6] P. Biecek: „Przewodnik po pakiecie R". Oficyna Wydawnicza GIS, Wrocław, 20017.
[7] P. Biecek: „Analiza danych z programem R. Modele liniowe z efektami stałymi, losowymi i mieszanymi". Wydawnictwo Naukowe PWN, Warszawa, 2013.
[8] M. Crawley: „The R Book". Willey-Blackwell, 2012.
[9] B. Everitt, T. Hothorn: „A Handbook of Statistical Analyses Using R". Chapman&Hall/CRC Computer Science & Data Analyses, 2010.
[10] M. Gągolewski: „Programowanie w języku R. Analiza danych, obliczenia, symulacje". Wydawnictwo Naukowe PWN S.A., Warszawa, 2016.
[11] C. Gillespie, R. Lovelace: „Wydajne programowanie w R. Praktyczny przewodnik po lepszym programowaniu". APN Promise, Warszawa, 2018.

Design and construction of a model of an undershot hydroelectric power plant

inż. Dawid Szkyrpan
ORCID No.: 0009-0001-4289-9443; e-mail: dawid94102@wp.pl
Stanisław Staszic State University of Applied Sciences in Piła,
Department of Mechanical Engineering

1. Introduction

Energy sourced from flowing water is one of the main renewable energy sources that humans have been using for their needs since ancient times. Water-power plants, as a consequence of the water mill concept, have existed in the energy sector for many years.

In hydroelectric power plants, electrical energy is obtained as a result of converting the potential energy of water into mechanical energy in a turbine and through generators - into electrical energy [19].

Hydropower is an ecological method of producing electricity. In Poland, before World War II, hydroelectric power plants were the main sources of cheap energy. They included mills, water pumps, fulling mills, and sawmills [21].

Water mills were among the first hydrotechnical structures. In Poland their construction began at the turn of the 11th and 12th centuries and became widespread in the 13th century. At first these were systems powered by a single water wheel which was used in order to move stones that ground grain. Since the 16th century, several wheels were installed in the mill facilities. Until the beginning of the 20th century, water mills were the basic solution for the management of small rivers. Their role was economic and they constituted the beginnings of industrial plants. Moreover, they influenced changes in the geoecosystems of river valleys [5].

The introduction and increasingly widespread use of the water mill was a revolutionary breakthrough, not only from the perspective of grain grinding. The elimination of household millstones and their replacement with millstones powered by water power was a civilizational progress, especially since the efficiency of these devices exceeded human labor. The construction of water mills also had an impact on long-term changes in water relations in river valleys [4].

In the pre-industrial period, fast-flowing water streams were also used to create other water-powered devices. Used for grinding grain, cutting wood (sawmills), producing cloth (fulling mills), driving bellows in forges (forges) and crushing bark (oak mills in tanneries). Initially, self-acting backwater and mill wheels were used to power installations in mangles, starch mills and weaving mills [19, 21]. The great variety of these devices means that the term "mill" includes all devices whose main drive is a shaft rotating around its own axle, regardless of the forces that move it [11].

The principle of operation of water mills did not change substantially from the Middle Ages to the mid-19th century. At that time observed was a principle that a single driving mechanism (water wheel) powered a single working system, i.e. a set of millstones or mortisers. Mortisers (or groats mortars) usually consisted of a stone bowl or a hollowed-out wooden block and a pestle or beater (an elongated stone or wooden stick) and were used for hulling or grinding grain [24]. Yet another method was to use appropriate water wheels. For example, until the interwar period, the mills in the Szadków region were powered by undershot and overshot wheels. Also, midshot wheels were used[17].

The heart of the mill was the water wheel which was built of oak wood, 0.5 to 1 meter wide and up to 3 meters in diameter. They were attached to the end of the main shaft, protruding from the side wall of the mill situated above the water. The shaft rested on thick supports made of bearing beams. It was built of hard oak wood resistant to abrasion and mechanical loads. Its diameter was approximately 0.5 meter due to the transfer of the rotational motion of the wheel into the mill inside. The main wheel was equipped with protruding pins or wedges, hence its name: fingerlike. The pins, when rotated, engaged with the protruding parts, or rods, which formed the coil, or hexagon. The coil also included ferrules - two discs of different diameters, fastened one above the other, overlapping each other with diagonal coils (fingers). The ferrules were placed on a common vertical axle, i.e. the spindle. This is how a simple gear was created, transferring the rotary motional of a shaft with horizontal axle of rotation to the rotational motion of coil with a vertical axle of rotation. The wooden, and later steel, spindle was placed at its lower end in a socket located on a horizontal beam. The upper end was attached to a three-armed steel piece (forked iron bar), located in sockets, i.e. grooves in the eye of the upper millstone (the upper, movable millstone with the mounting of the rotating mechanism). When activated, the forked iron bar caused the rotational motion of the upper millstone. This is where the grinding mill was, the key - after the water wheel - part of the mill. The grinding mill consists of two stones, lower and upper, with diameters ranging from 700 to 1000 mm, operating in a fixed wooden casing. The lower, stationary stone, the so-called "bed stone", was smooth, and the working part of the movable upper stone, the "runner", was cut with oblique grooves. Their role was to gather and grind the grain which was pushed by centrifugal force to the outer edges of the stones. Millstones wore out quite quickly. They were sharpened on average once every 7 days. And then grooves were cut on the grinding part [45].

The working properties of water mills meant that their location and architectural structure were submitted to the river. The water should have had a significant flow but it was not necessary to build a mill on the river bank. Sometimes the mill was built between anchored rafts, on barges or floats, whose position along the current was maintained by ropes wound around a windlass located on the shore. This is how mills - called boat mills or floating mills, quite common in the 15th century, were built. Mills were also built on "scales", i.e. on piles driven into the riverbed and connected to the bank by a wooden platform. Mills in mountainous areas were built quite early; there fast-flowing streams provided sufficient energy to turn the mill wheels. The vast majority of mills were made of wood, sometimes with an addition of a foundation attached to the shore. If the wall with the water wheel extended beyond the shoreline, thick oak piles were fitted underneath and driven into the river bed. Large monasteries and wealthy cities built brick mills, equipped with several water wheels, each of which moved separate millstones. In Barbegal (France), in the 4th century there was a complex of mills consisting of 16 water wheels [29].

2. Types of water wheels

The position of wheel axle can be taken as the criterion applied for the division of water wheels. This category has two different types of wheels, including horizontal-axle wheels and vertical-axle wheels, which are shown in Fig. 1÷2.

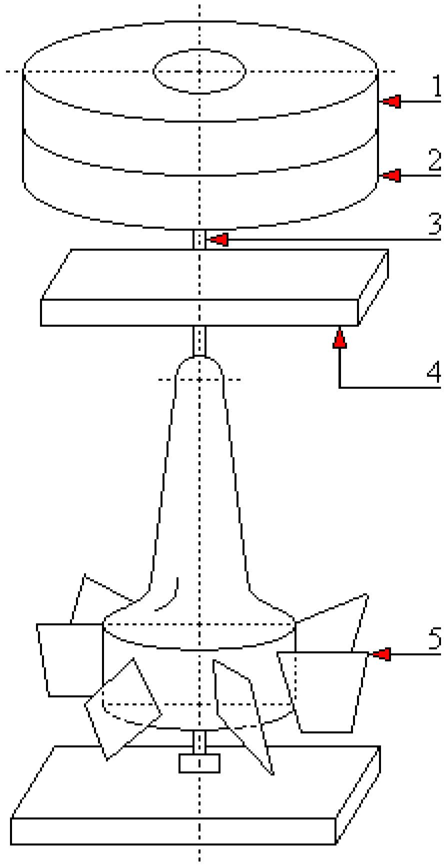

Fig. 1. Schematic diagram of the construction of a water wheel with a vertical axle
1-upper millstone; 2-lower millstone; 3-axle transmitting power; 4-base for mounting the water wheel; 5-water wheel

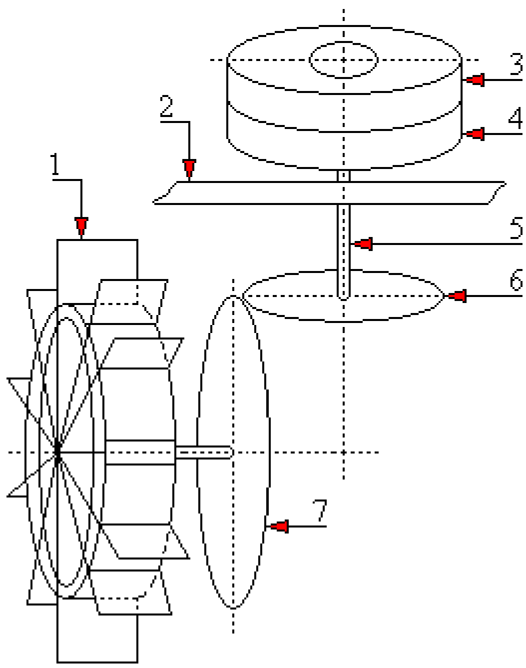

Fig. 2. Schematic diagram of the construction of a water wheel with a horizontal axle
1–water wheel; 2–mill floor; 3–upper millstone; 4–lower millstone; 5–axle transmitting power; 6–passive (driven) finger wheel; 7–active (driving) finger wheel

Original water wheels with horizontal crushers already existed in the 1st century BC in the Roman Empire. We have this information because the court architect of Emperor Octavian Augustus - Marcus Vitruvius (Vitruvius) Pollio included a lot of information about them in his own work - "Architecture" from 25-23 BC. The mill with a water wheel with a horizontal axle, which was the subject of his work, had a gear transmission thanks to which a concave-rimmed millstone located on the second vertical cylinder operated. In the literature, the presented type of mills are referred to as Roman mills, and one can also find the name Vitruvius mill. It is believed that in the earlier past there were mills with water wheels located on a vertical shaft with a concave-rimmed stone. These simple solutions had an impeller that rotated in a horizontal plane, and water was led to it through a pipe with a sharp inclination. The rotors were water wheels of the spray type. The water hit a series of half-bowls or diagonal boards located around their circumference (as can be seen in Figure 3). In the literature examining the history of milling and the use of water power, the presented type of mills is referred to as Turkish or Greek mills, as well as turbine mills. It is suspected that they originated in Asia Minor, and today they can still be found in Anatolia in present-day Türkiye [33].

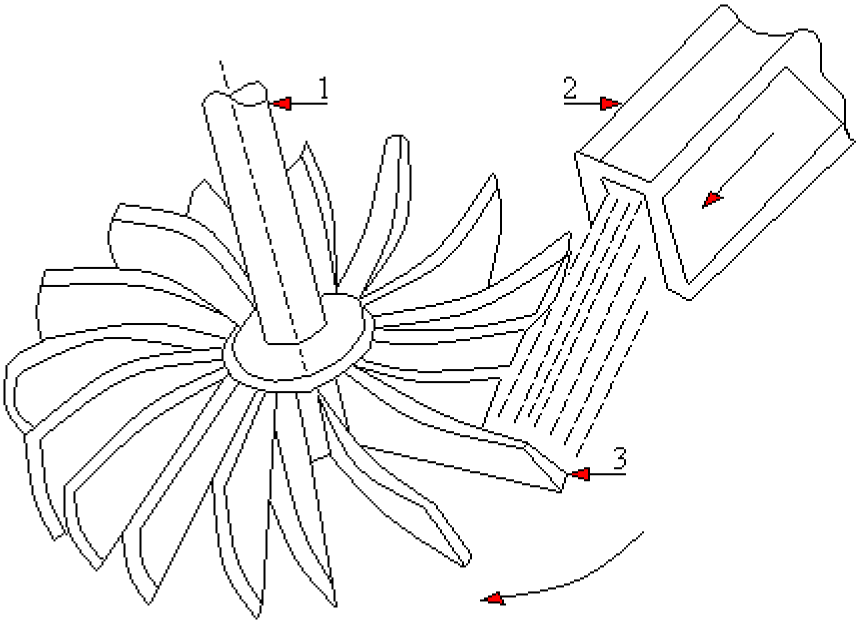

Fig. 3. Spray water wheel
1-paddle wheel shaft; 2-water supply chute; 3-wheel paddle blades

In Poland, in Podhale region, there is another type of water wheel called the Vlach wheel (Fig. 4).

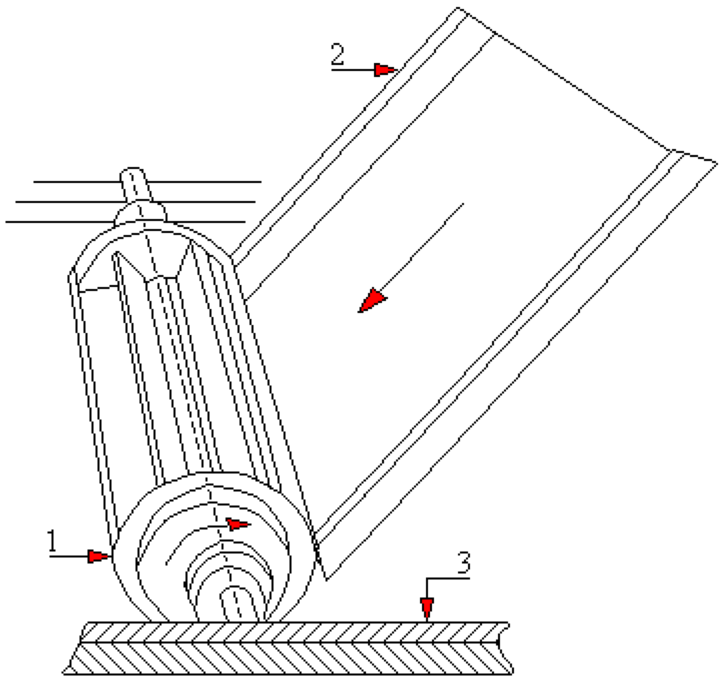

Fig. 4. "Vlach" type water wheel
1–water wheel; 2–water supply flume; 3–water wheel mounting wall

Taking into account the situation of the horizontal axle wheels based on whether the water jet falls on the water wheels from above, the following designs are distinguished: overshot, midshot and undershot shown in Fig. 5÷ 7 [15].

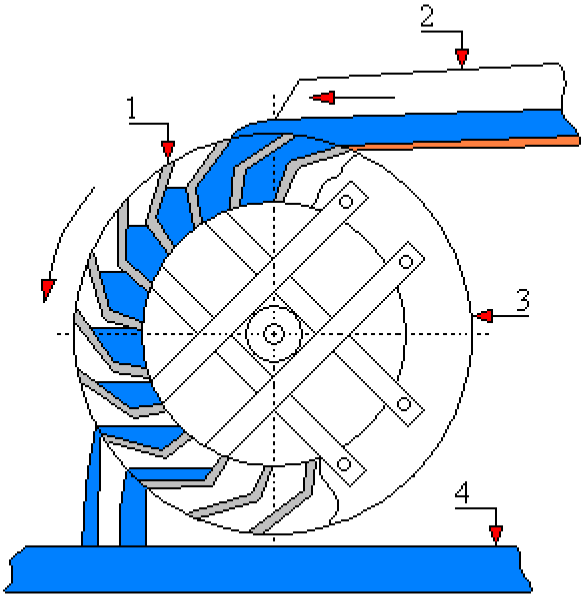

Fig. 5. Diagram of the construction and operation of an overshot water wheel
1-water wheel paddle blades; 2-water supply chute; 3-water wheel; 4–lower water surface

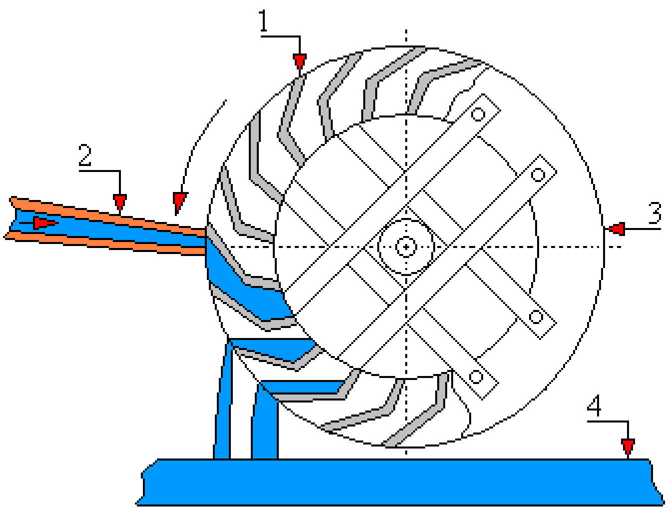

Fig. 6. Diagram of the construction and operation of a mid-shot water wheel
1-water wheel paddle blades; 2-water supply chute; 3-water wheel; 4–lower water surface

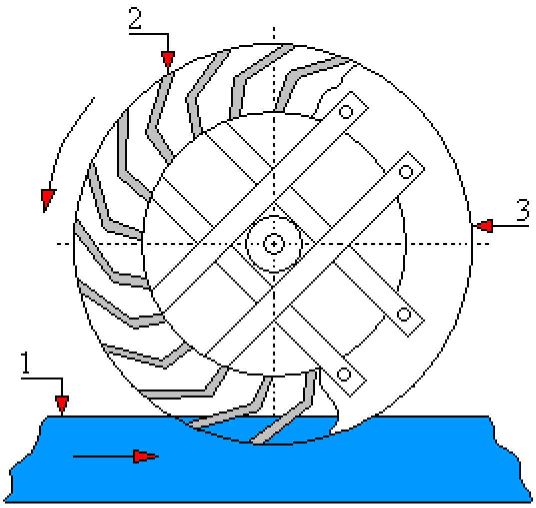

Fig. 7. Diagram of the construction and operation of an undershot water wheel
1–water jet; 2–water wheel paddle blades; 3–water wheels

The presented types of wheels differ in their efficiency [32, 16, 18]. Overshot wheels (Fig. 5) use primarily the potential energy of water. Their specific feature is their increased efficiency estimated at about 60% because the accumulated backwater falling freely has much greater energy. The overshot wheel can be used for operating on rather small streams, where the flow rate is low, but the level difference is still maintained, thanks to which greater efficiency can be obtained from a small water flow rate. Water is transported via a trough to the paddles on the wheel, and the water is collected in cells that have been generated by side walls of the wheel and paddles. The weight of the water causes the wheels to turn and as the cells are slowly emptied, which occurs due to rotation, the water slowly flows out into the stream on the outflow side. The water flowing into the wheel is directed by movements of a manual valve. The wheel should be placed above the bottom water.

The undershot water wheel uses primarily the kinetic energy of water. This type of wheels is characterized by low efficiency, estimated at 22%. An undershot water wheel is a wheel with a horizontal axle and is similar to an overshot wheel, and it rotates under the influence of water hitting the paddle blades on the lower side. When comparing the overshot wheel with the undershot wheel, the latter uses significantly less hydraulic engineering input during assembly (this is related to transporting water to the lower part of the wheel). The flow rate and associated power are regulated by a valve located directly in front of the wheel. The gate valve causes the speed of the water hitting the paddle blades to increase – a significant fraction of the hydraulic energy is converted into kinetic energy.

A type of undershot wheel is called a stream wheel in a situation where the bottom of the flume remains (almost) horizontal. The wheel paddle blades are pushed by the flowing water and in this situation its speed is reduced. The radial dimension of the paddle blade is greater than the depth of water in the flume. The mechanical energy of the stream wheel is obtained from the kinetic energy of the water. This type of wheel is not as efficient as the classical undershot wheel. The power obtained from the flowing water is the same as the difference in kinetic energy fluxes both in front of and behind the wheel.

Midshot wheels use the potential energy and kinetic energy of water. Wheel efficiency is estimated at approximately 50%. A midshot water wheel is powered by water that is located slightly below its axle. The flume responsible for conducting water has a curved shape that matches the curvature of a circle. This creates a radial gap with a width of 12 to 25 mm, and its role is to reduce leaks. A flume shaped in this way is made of concrete, plastered bricks, steel sheets, and sometimes even wood is used. It is worth remembering that all solids floating on the water surface should be separated from the water as they may be responsible for wheel paddle blade failure. Midshot wheels are not as efficient as overshot wheels but they work much better than undershot wheels. The paddle blades of the midshot wheel have a rounded profile, as do almost all overshot wheels, which distinguishes them from undershot wheels which have straight paddle blades.

3. **Design of a model of the undershot hydroelectric power plant**

The aim of this work is to prepare a model presenting physical properties of an undershot wheel used as a voltage generator.

Basically, the design of the hydroelectric power plant in question is based on a mounted wheel where the flowing water hits the paddle blades at the bottom of the wheel, setting them in motion. The paddle blades, in turn, set the wheel in rotational motion. The design of such a power plant is the least efficient and is probably the oldest method of obtaining electricity using renewable energy sources. However, the described construction also brings the advantage of cheap construction of such a power plant. To obtain enough energy, this type of power plant should be used in places where the water flow is high which will result in obtaining high wheel torque.

4. **Development of design variants**

When designing the model of the undershot hydroelectric power plant various design variants presented below were adopted.

First variant (Fig. 8)

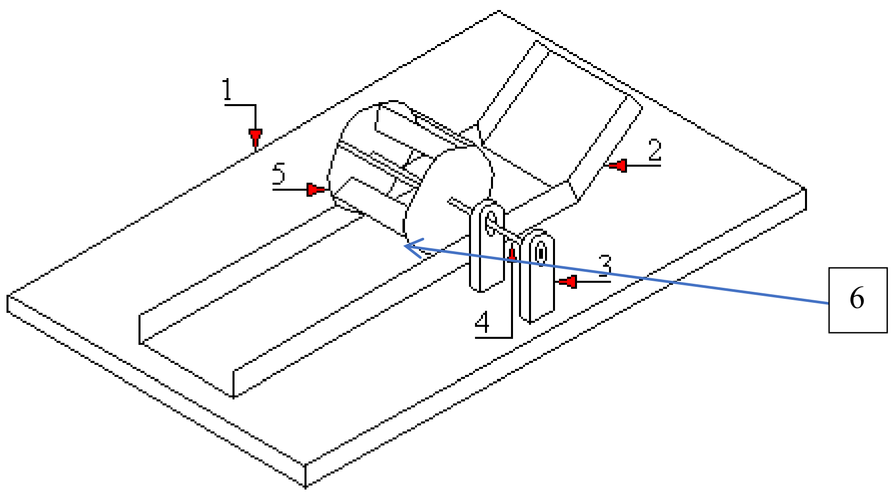

Fig. 8. First variant of the model design
1-model base; 2-chute; 3-shaft support base; 4-drive shaft; 5-water wheel

A water wheel mounted on a shaft supported on one side by two supports, the shaft not supported at one end, the water would flow down the chute hitting the wheel paddle blades.

The second variant is a wheel mounted on a shaft supported on both sides at each end, the water would flow under the wheel in a chute.

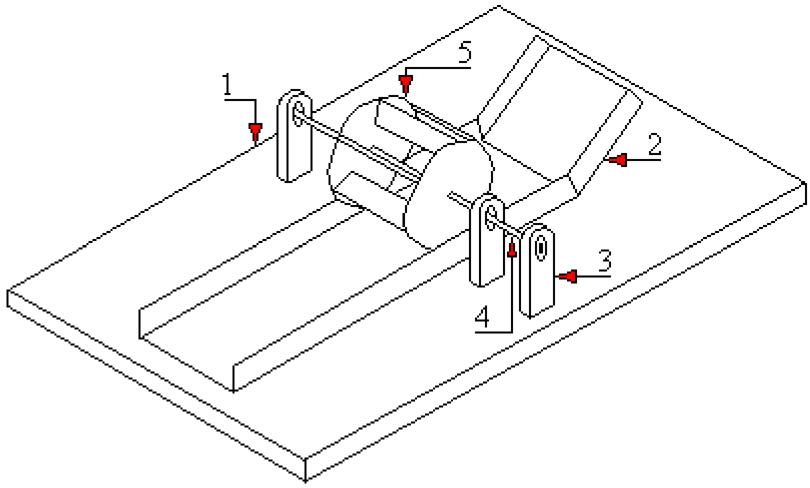

Fig. 9. The second variant of the designed model
1-model base; 2-chute; 3-shaft support base; 4-drive shaft; 5-water wheel

The second variant (Fig. 9) is a wheel mounted on a bearing-mounted shaft and supported on both sides at each end, the water would flow under the wheel in the chute. The third variant (Fig. 10) is the construction of a water turbine in a closed housing with a wheel mounted on a shaft supported on bearings on both sides, the water wheel is connected by means of a drive belt moving on two pulleys, water is supplied to the turbine directly from the water source by means of pipes and a hose. The water is drained via a drainpipe to a separate tank.

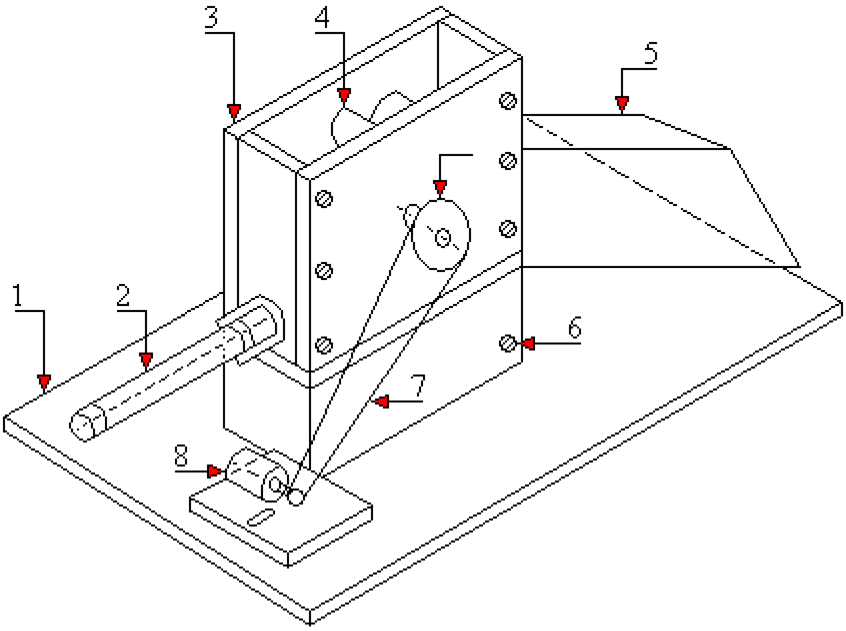

Fig. 10. The third variant of the designed model

1–device base; 2–water supply pipe; 3–housing; 4–water wheel; 5–water drainage chute; 6–mounting screw; 7–transmission belt; 8–power generator

The third variant with a water wheel in a closed housing was selected for implementation. The third variant was chosen due to its relatively simple construction and the fact that during tests the area around the turbine was not splashed with water, which is a great advantage for this model and for showing how the turbine works. Another aspect is its simple construction, easy assembly and disassembly. The drive from the turbine is transferred by means of a drive belt moving on pulleys, which gives us a higher speed ratio on the generator. The model was mainly designed in Autodesk Inventor 2017.

5. **Design and construction of the model**

The design of the test ring enables testing of the operation of an undershot hydroelectric power plant in various operating conditions; the model enables us to check the influence of the speed and intensity of flowing water on the operation of such a power plant and check its efficiency. Tests were carried out at different water flow rates and measurements were taken on individual elements of the model. The model allows us to measure the voltage generated by the generator, measure the number of revolutions on individual pulleys, measure the water pressure before the valve regulating the amount of water flowing, and measure the amount of water supplied to the model. The drive unit was mounted on a 5mm diameter shaft, then the shaft was mounted in the housing on two bearings selected for the shaft diameter.

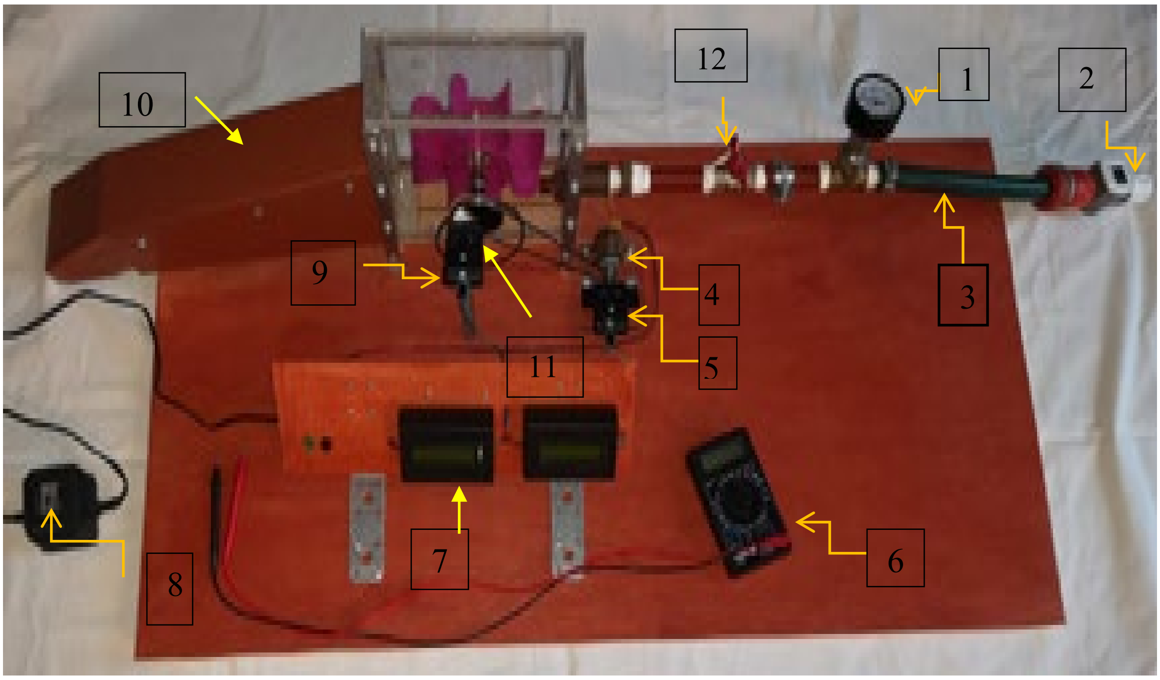

Fig. 11. Laboratory test ring of an undershot hydroelectric power plant
1-manometer, 2-water meter, 3-water supply hose, 4-power generator, 5-speed sensor, 6-multimeter, 7-control and measurement panel, 8-power supply (sensor power supply), 9-speed sensor, 10-chute, 11-speed sensor, 12-ball valve

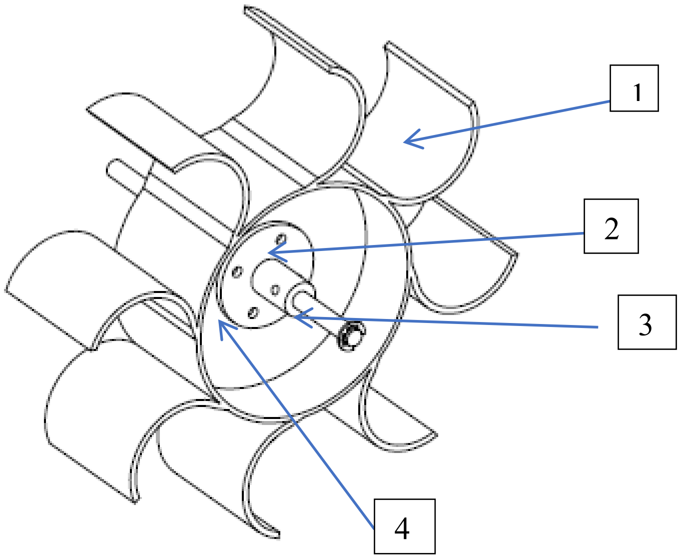

Fig. 12. Water wheel with shaft (drive unit)
1-water wheel, 2-shaft connector with wheel, 3-drive shaft, 4-M3 mounting screw

The drive unit consists of a water wheel connected to a shaft designed for the needs of the model. The whole thing was connected using M3 screws through mounting holes made in the individual parts.

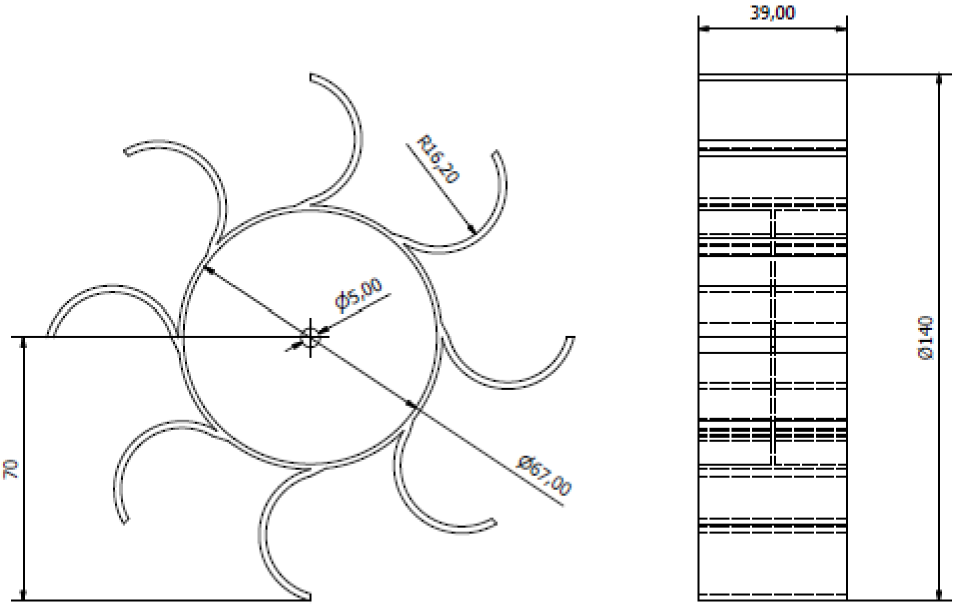

Fig. 13. Water wheel without shaft

The water wheel (Fig. 13) was used from a toy, but for the purposes of building the model it was modified to enable connection to the shaft. A 5 mm diameter hole was made through which the shaft passes, as well as four smaller 3 mm diameter holes for connection with the connector (Fig. 4.12).

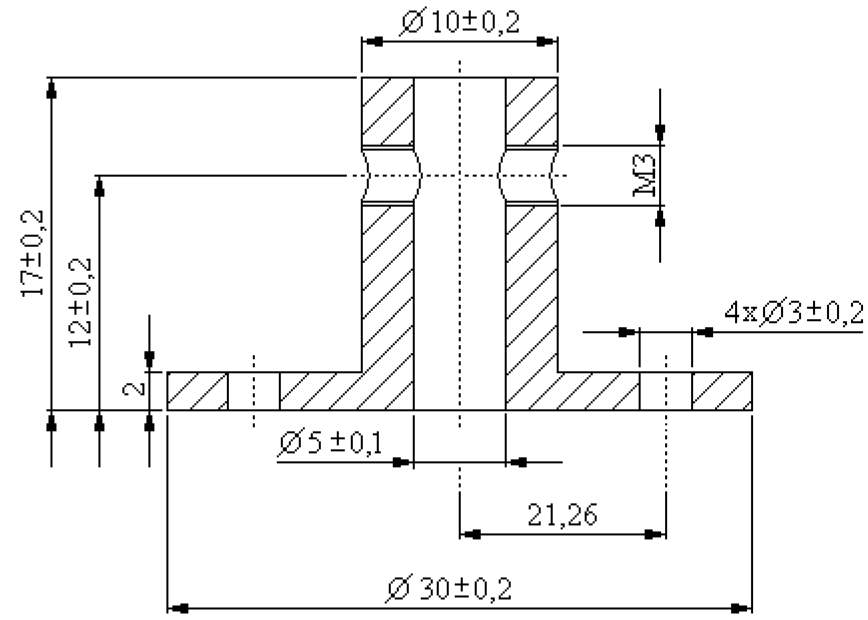

Fig. 14. Wheel to shaft connector

The water wheel to shaft connector (Fig. 14) is made of aluminum, with holes through which M3x10 screws go, connecting the wheel with the shaft into one drive unit.

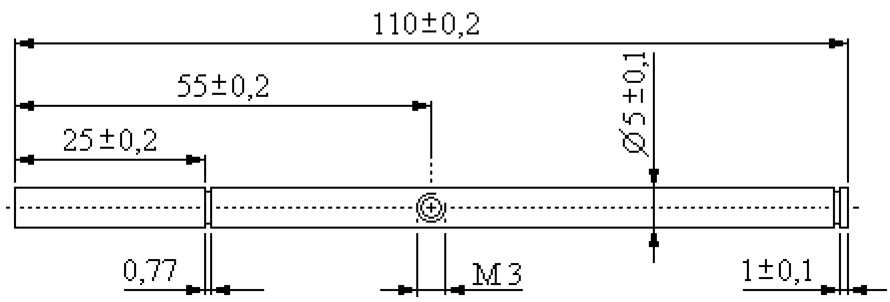

Fig. 15. Drive shaft

The drive shaft (Fig. 15) is made of steel with a visible mounting hole for connecting the drive unit using an M3x10 screw, and with visible 0.77 mm wide grooves. These grooves are used to position the drive unit in the turbine housing so that it does not move. The drive unit is set in one place using a retaining ring selected to suit the groove diameter, so that the entire unit does not move during operation. There are also two sealing rings on the shaft which seal the place where the shaft passes through the bearing.

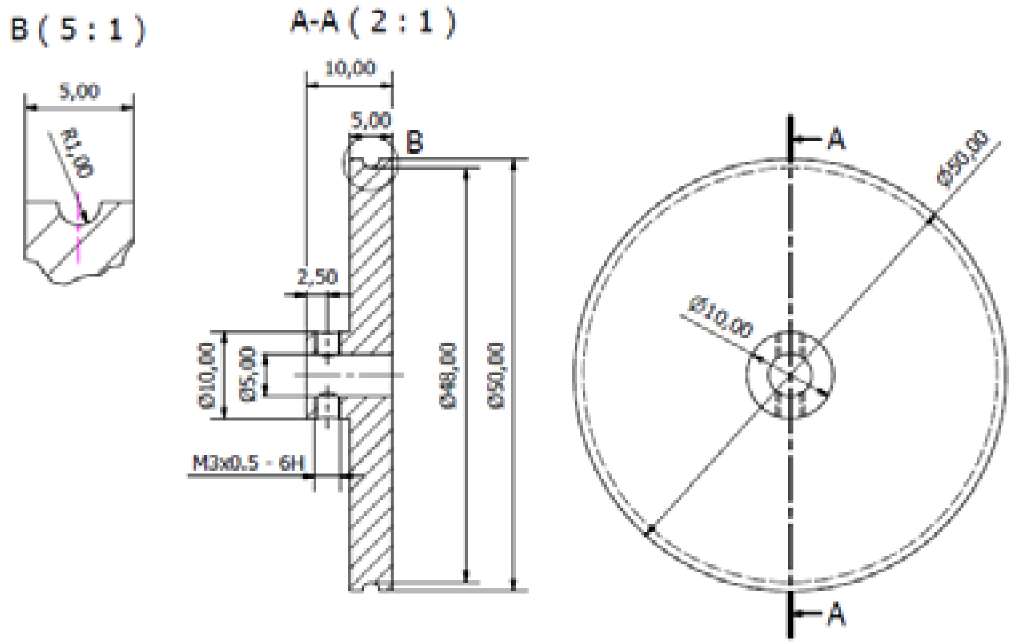

Fig. 16. Drive pulley

The drive pulley (Fig. 16) with a diameter of 50 mm is made of aluminium with a hole for mounting on the shaft using M3x4 set screws and a groove is made for a round drive belt.

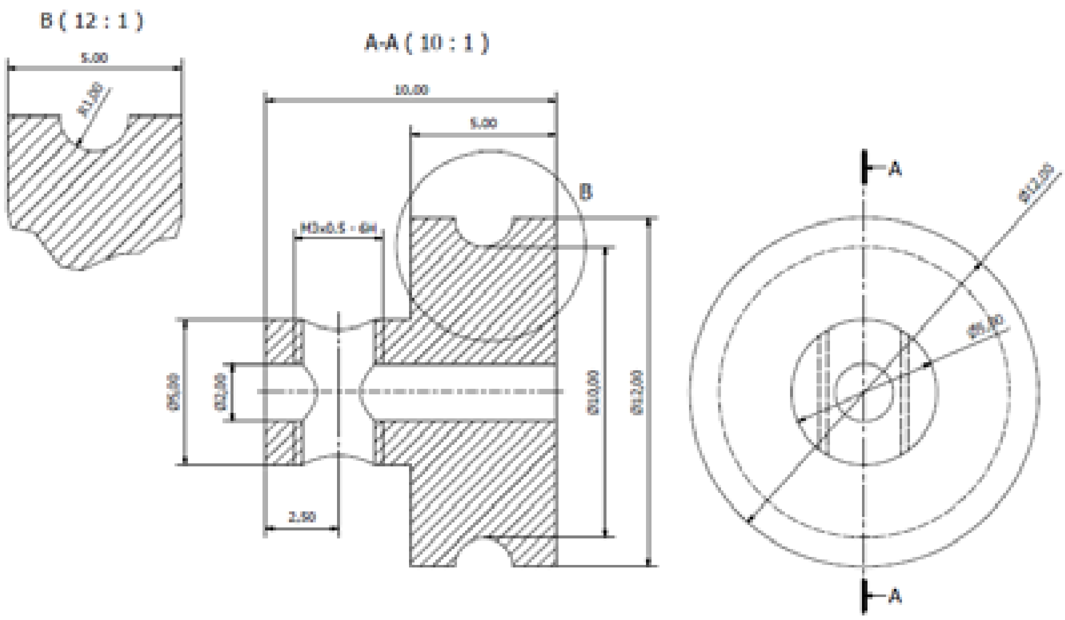

Fig. 17. Idler pulley

Idler pulley (Fig.17) with a diameter of 12mm was made of aluminum, the wheel was mounted on the generator on a 2mm diameter shaft using M3x4 set screws. A groove is made in the wheel for the round drive belt.

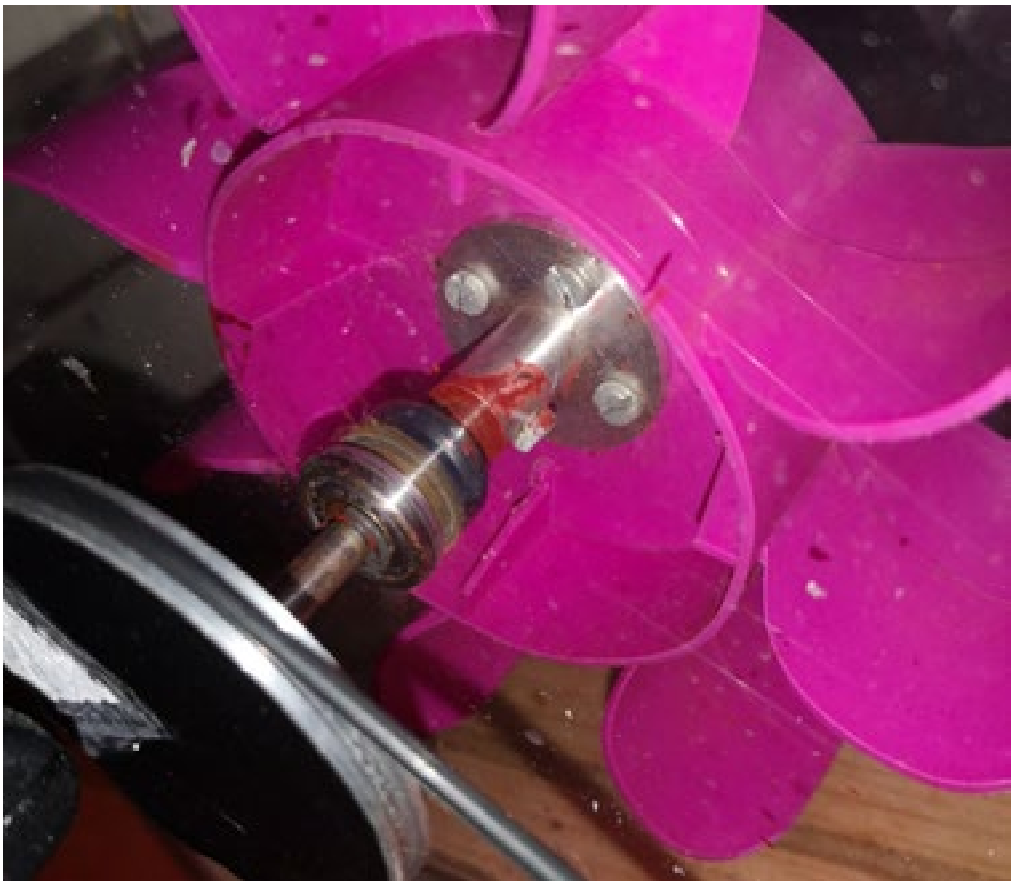

Fig. 18. View of the water wheel drive unit

To mount the water wheel taken was an EZO MR 105 2Z ball bearing with increased clearance with the following parameters:

- inner diameter 5 mm;
- outer diameter 10 mm;
- width 3mm;
- clearance C3

To measure the number of revolutions, an AVT 1870 tachometer was used to measure the number of revolutions on individual pulleys using a transmitting and receiving diode. The wheels are covered with black foil with a white symbol on it thanks to which the signal sent from the transmitting diode is reflected from the white point to the receiving diode and after the signal is processed the display shows the number of revolutions in [RPM]. The parameters of the tachometer used are as follows:

- power supply: 8÷12V;
- reading of revolutions in [rpm] or in [rps];
- measurement accuracy: ±1 revolution per second;
- measurement in the range from 0 to 2999 rpm;
- a photoelectric sensor is used as the working element.

A generator with the following technical parameters was used as the current generator:

- output voltage: DC 0.01 ÷ 29.99 V;
- output current: 0,0 ÷ 100 mA;
- rated speed: 100 - 6000 rpm;
- generator diameter: 24.5 mm;
- generator height: 34.2 mm;

- motor shaft diameter: 2 mm;
- motor shaft length: 13.5 mm

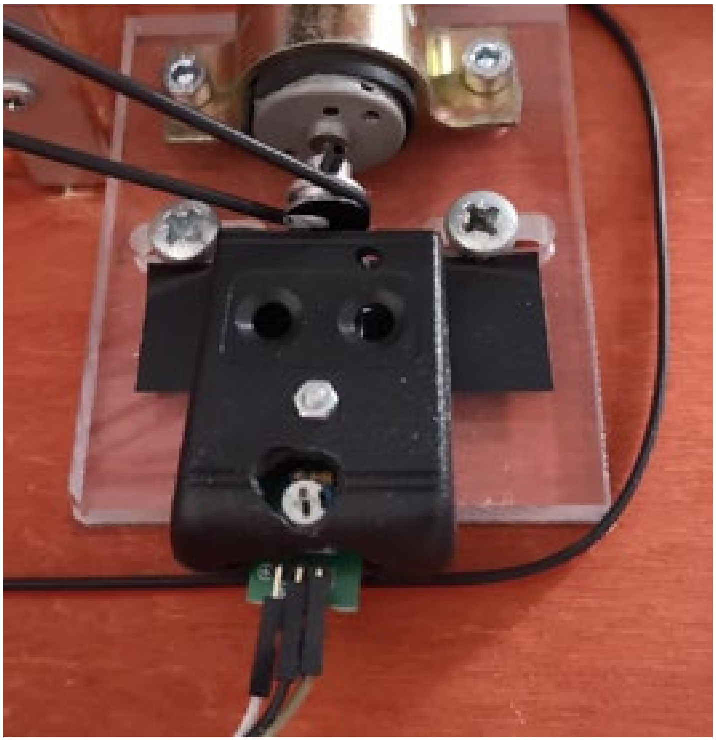

Fig. 19. View of the sensor measuring the rotational speed of the driving wheel and the generator

The speed measuring devices are built in such a way as to protect the electronics against damage and against interference from external factors.

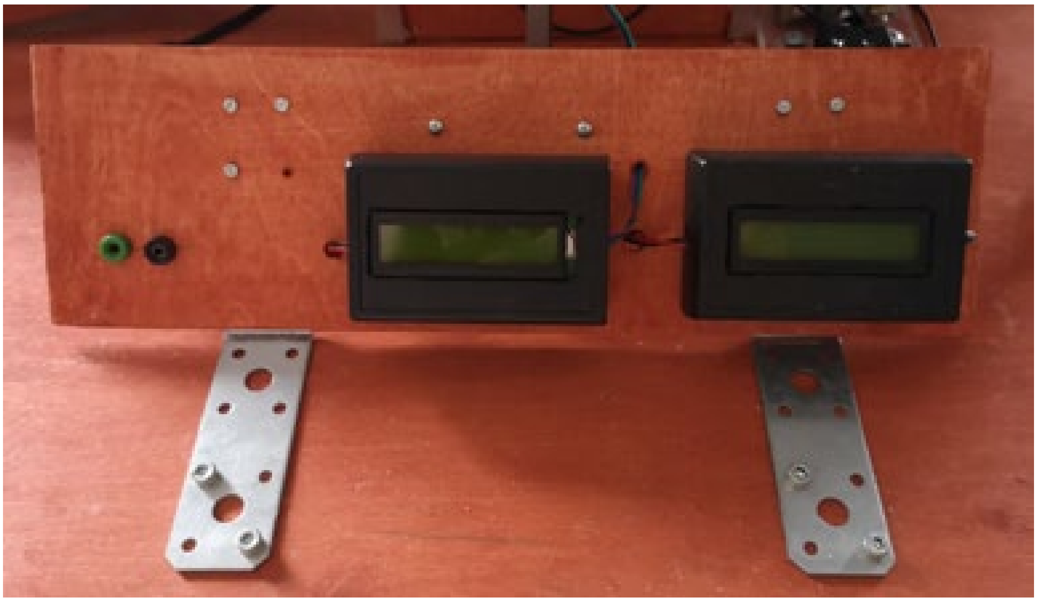

Fig. 20. View of the measuring panel with AVT type tachometer display units for the driving and idle wheels

The measuring panel (Fig. 20) features tachometer display units and electrical sockets, so-called banana sockets, connected to the generator, to which we can connect a meter and measure the generated voltage or connect a diode or a light bulb.

Fig. 21. View of the enclosed water drainage chute and water turbine

The chute (Fig. 21) was made of sheet metal, appropriately bent. The chute effectively drains water to a separate tank placed lower down, the chute is made of two parts and properly inserted one into the other so the whole thing is tight.

The water turbine housing is made of 10 mm thick plexiglass. This material was chosen because it allows for viewing the model in action. The side walls of the model have holes in which the bearings are mounted, and a pipe with a narrowed end passes through the front wall so that the flowing water has greater speed and pressure. The whole thing was screwed together using M5x15 screws through an aluminum flat bar, and additionally sealed with colorless silicone. The entire housing is mounted on a wooden beam and screwed to the base.

A ½" butterfly ball valve was installed and connected to the ½" pipes. The threaded connections were appropriately sealed with Teflon tape. The valve is used to regulate the amount of water supplied to the water wheel, thanks to which we can regulate the amount of water flowing.

Fig. 22. White Line 3100 Water Flow Meter

Properties of the meter shown in Fig.22:

- Upper counter- single flow volume;
- Bottom counter- total volume of water flow;
- Clear button - zeroing the total measurement;
- Reset button - zeroing the total measurement;
- Measurement tolerance:

- working pressure: 1 ÷ 2 bar and 9-10 bar: +/- 10%
- working pressure: 3 ÷ 8 bar: +/- 8%

The device shown in Figure 22 allows for measuring water flow up to 999.9 liters/gallons of water per minute. By default, the meter unit is a liter. The device is battery powered. It turns off automatically after approximately 30 minutes if not used.

By using a ½ to 3/8 hexagonal reducing pipe we obtain higher water pressure at the outlet and higher speed. This has a positive effect on the operation of the turbine, increasing its efficiency.

6. **Calculations**

Strength calculations for the shaft were performed in Autodesk Inventor 2017

Table 1. Material properties used for calculations

Material		Steel
Elastic modulus	E	206000 MPa
Shear stress modulus	G	80000 MPa
Density	ρ	7860 kg/m^3

In Table 1 shows the properties of the material from which the shaft was made and what coefficients were taken into account during the calculations.

Table 2. Load values

Loads											
	Position	Transverse force				Torque	Deflection [micrometer]				De-flection angle [deg]
		Y	X	Volume	Direction		Y	X	Volume	Dire-ction	
1	3 mm		10 N	10 N	90 deg		-0,379	-124,652	124,652	269,83 deg	0,18
2	75 mm					200,000 N m	0,030	14,167	14,167	89,88 deg	0,00
3	75 mm					-200,000 N m	0,030	14,167	14,167	89,88 deg	0,00
4	105 mm	8 N		8 N			-0,000	0,000	0,000	180,00 deg	0,04

In Table 2 shows the load values that were taken into account during the simulation and distribution of loads on individual axes, the force assumed on the X axis = 10N and on the Y axis = 8N, the assumed torque is 200N, in the deflection columns shown are individual results for each axis.

Table 3. Value of reaction at supports

	Support type	Position	Reactive force				Deflection [μm]				Defle-ction angle [deg]
			Y	X	Volume	Dire-ction	Y	X	Volume	Direction [deg]	
1	Free	51mm	0,154 Nm	18,889 N	18,90 N	89,53 deg	-0,00	0,00	-0,000	180,00	0,08
2	Fixed	105mm	8,012 Nm	-8,889 N	11,967 N	312,03 deg	0,00	0,00	0,000	180,00	0,04

Table 3 presents the value of reaction at supports for individual axes X and Y, the value of forces for the fixed and movable support, and the value of deflection.

Table 4. Calculation results after strength simulation

Type of tested quantity	Result
Length L	110.000 [mm]
Mass	0.017 [kg]
Maximum bending stress σ_B	39.114 [MPa]
Maximum shear stress τ_S	1.246 [MPa]
Maximum torsional stress τ	0.000 [MPa]
Maximum stress σ_T	0.000 [MPa]
Maximum reduced stress σ_{red}	39.124 [MPa]
Maximum deflection f_{maks}	134.243 [µm]
Torsional deflexion angle φ	0.00 [deg]

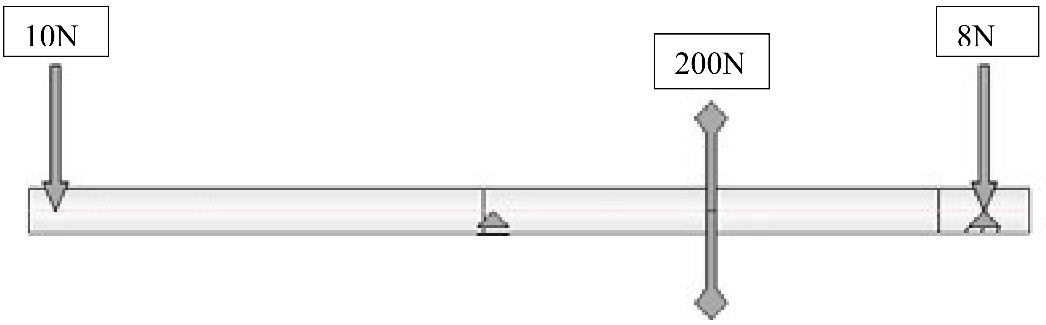

Fig. 23. Distribution of forces assumed in calculations

Fig. 23 shows a graphical representation of forces assumed in the computer simulation.

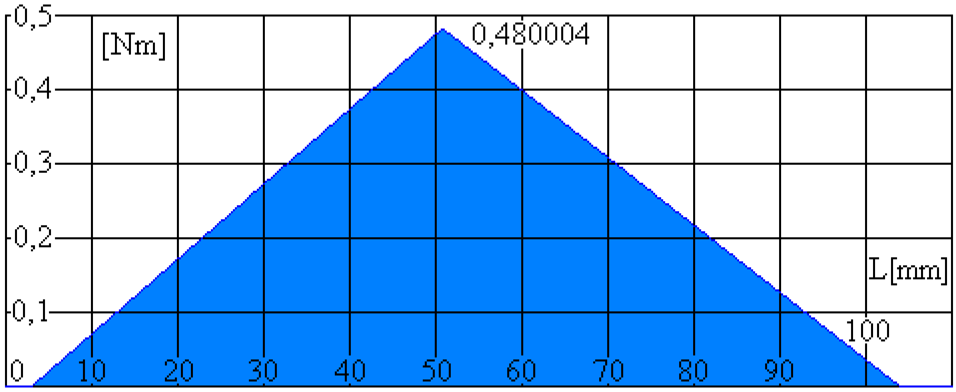

Fig. 24. Bending moment Mg [Nm]

Fig. 24 shows the value of the bending moment change, the maximum value of the bending moment is approximately 0.48 Nm in the XY plane.

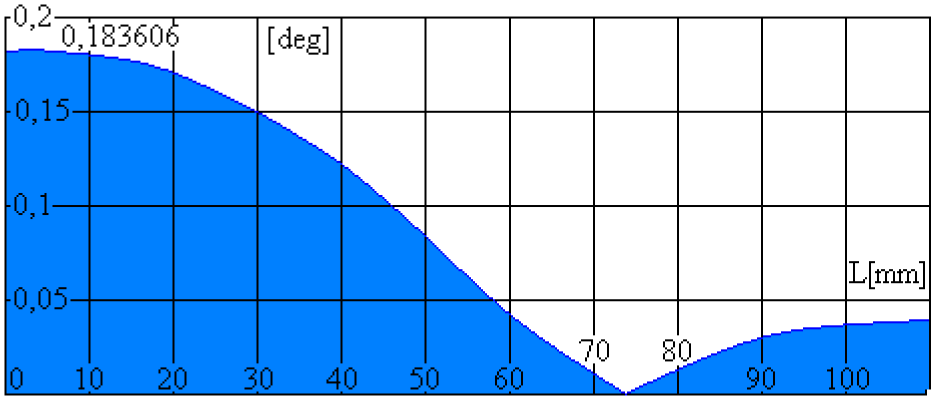

Fig. 25. Shaft deflection angle in the XZ plane

Figure 25 shows the shaft deflection angle at individual distances, the maximum deflection angle is approximately 0.18° close to the point where the force is applied. The largest deflection angle at this point is caused by the lack of support and the force acting at this point.

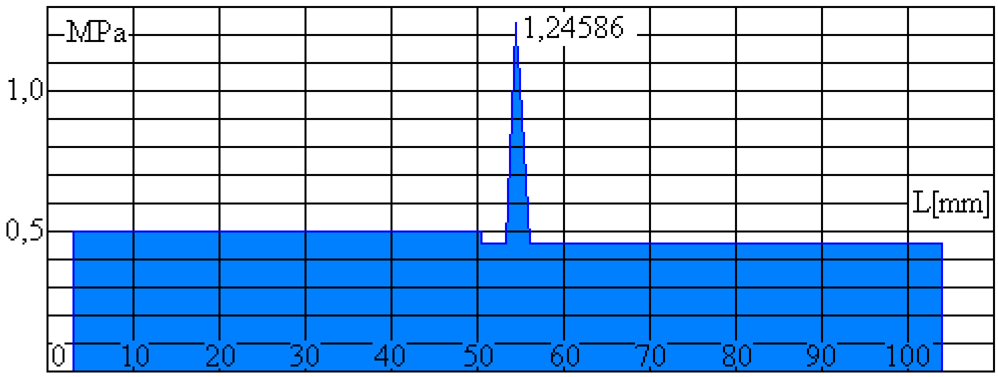

Fig. 26. Shear stresses

Fig. 26 shows a diagram of the shear stresses in the shaft. One can read that the stress is relatively constant at 0.5 MPa except for one peak of the value of ca. 1.25 MPa.

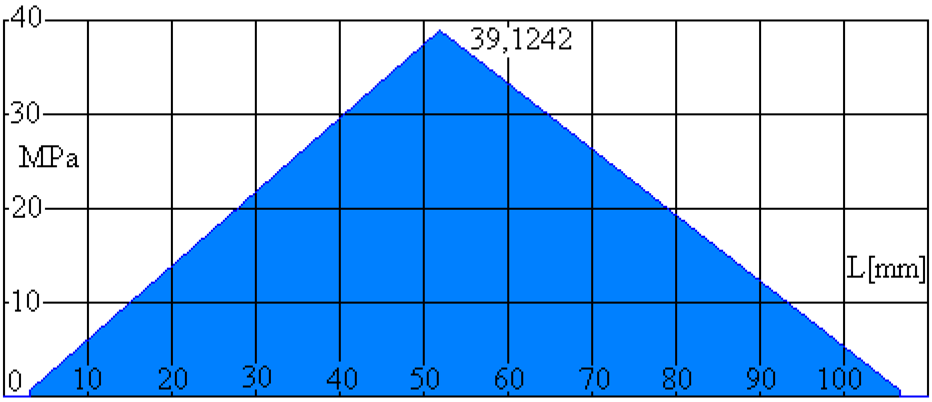

Fig. 27. Reduced stress

Fig. 27 shows a graph of reduced stress, the highest value of which is ca. 39 MPa.

7. **Testing**

The geometric ratio of the belt transmission is given by the formula:

$$it = \frac{d_1}{d_2}$$

d_1- driving wheel diameter; d_2 -driven wheel diameter; d_1 = 50 [mm];
d_2 = 12 [mm]

$$it = \frac{50}{12} = 4,166$$

The device testing was conducted in 3 stages. The first stage is a test with the valve fully open. The second stage - test with the valve open at 1/2 of its maximum position. The third stage - test with the valve open at 1/3 of its maximum position. Each test lasted 60 seconds, and measurements were recorded every 10 seconds. Number of repetitions: 10. The measurement tables are presented below. The pressure in the water supply network was 4.5 bar.

Test with a fully open valve

Table 5. Average measurement value for full valve opening (Test No. 1)

Number of revolutions of the big wheel [RPM/min] n_1	Number of revolutions of the small wheel [RPM/min] n_2	Voltage Generated [V]	Water flow rate [liter/min]	Kinematic transmission ratio $ik=n_2/n_1$
360	1560	5.73	20.6	4.33

Test with the valve open at 1/2 of its maximum position

Table 6. Average measurement values for 1/2 valve opening (Test No. 2)

Number of revolutions of the big wheel [RPM/min] n_1	Number of revolutions of the small wheel [RPM/min] n_2	Voltage Generated [V]	Water flow rate [liter/min]	Kinematic transmission ratio $ik=n_2/n_1$
360	1500	5.54	20.1	4.17

Test with the valve open at 1/3 of its maximum position

Table 7. Average measurement values for 1/3 valve opening (Test No. 3)

Number of revolutions of the big wheel [RPM/min] n_1	Number of revolutions of the small wheel [RPM/min] n_2	Voltage Generated [V]	Water flow rate [liter/min]	Kinematic transmission ratio $ik=n_2/n_1$
115	480	1.99	13.5	4.17

The more the water valve is open, the greater the amount of water flowing, the greater the voltage generated and the greater the slippage in the belt transmission.

7. Summary

An idea for further modernization of the model could be to modify the constructed test rig so that one model could meet the conditions of an undershot, midshot and overshot power plant by using appropriate bypasses, and the selection of the type of power plant could be done by using valves which would close the water flow and use a closed water circuit in order to save water and determine the effect of accumulated backwater (e.g. in a tank with adjustable height).

8. Literature

[1]. Baranowski B., Polskie młynarstwo, Ossolineum, Wrocław–Warszawa–Kraków–Gdańsk 1977, s. 137.
[2]. Bartnik A., Bartnik D., Rozmieszczenie młynów wodnych na obszarze Łodzi w świetle wykorzystanych historycznych źródeł kartograficznych, Z dziejów kartografii 21/2017, s.12.
[3]. Bednarska A., Hydroenergetyka w Polsce – obecna sytuacja i perspektywy na przyszłość,[w:] Bednarska, Hydroenergetyka w Polsce – obecna sytuacja i perspektywy na przyszłość(31.07.2018), s. 2
[4]. Brychcy D. Kaniecki A., Średniowieczne młyny wodne i ich wpływ na przemiany stosunków wodnych na przykładzie zlewni Obry Skwierzyńskiej, Badania Fizjograficzne 61/2010, s. 145-146
[5]. Brykała D., Uwarunkowania przyrodnicze lokalizacji młynów wodnych w zlewni Skrwy, Problemy Ekologii Krajobrazu 10/2001,s.164
[6]. Cieśliński R. Kowalczyk,, Analiza potencjału hydroenergetycznego oraz możliwości jego wykorzystania w województwie pomorskim, Woda-Środowisko-Obszary Wiejskie 18(1-61)/2018, s. 70
[7]. Drobniak S., Kowalewski T. A., Mechanika płynów – dlaczego tak trudno przewidzieć ruch płynu?, IMC Politechnika Częstochowska, IPPT PAN, Warszawa 2010, s. 389.
[8]. Dyrektywa Parlamentu Europejskiego i Rady 2009/28/WE z dnia 23 kwietnia 2009 r. w sprawie promowania stosowania energii ze źródeł odnawialnych (OZE)
[9]. Dyrektywa 2000/60/WE Parlamentu Europejskiego i Rady z dnia 23 października 2000 r. ustanawiająca ramy wspólnotowego działania w dziedzinie polityki wodnej
[10]. Energia ze źródeł odnawialnych w2016 r., GUS, Warszawa 2017
[11]. Górzyńska A., Górzyński T., Majewski M., Późnośredniowieczny młyn z Mniszka na ziemi świeckiej ze stanowiska 16, Raport Autostradowy 2005—2006.
[12]. Gutry-Korycka M., Pociask-Karteczka J. Sadurski A.., Skrzypczyk L., Zasoby wodne, wykorzystanie, zagrożenia stan obecny, tendencje, przyszłość, [w:] www.kbzw.pan.pl/images/stories/Rozdział _2. (31.07.2018), s. 1
[13]. Kalda G., Analiza stanu energetyki wodnej w Polsce, Czasopismo Inżynierii Lądowej, Środowiska i Architektury 61(4)/2014, s. 81
[14]. Kasperek E., Kasperek R. Wiatkowski M., Analiza możliwości budowy małych elektrowni wodnych na rzece Nysie Kłodzkiej. [w:] Cz. Rosik-Dulewska, M. Wiatkowski (red.), Zarządzanie kryzysowe – zrównoważony rozwój obszarów wiejskich, Uniwersytet Opolski, Opole 2010, s. 53–65
[15]. Koła wodne i turbiny. Samouczek Techniczny, Wydawnictwo Popularno Naukowe, Cieszyn 1923, s.7
[16]. Kucharski R., Lamprecht M., Młynarstwo regionu szadkowskiego i jego rozwój do I wojny światowej, Biuletyn Szadkowski 5/2005, s. 71-72;
[17]. Kucharski R., M. Lamprecht, Młynarstwo regionu Szadkowskiego i jego rozwój do I wojny światowej, Biuletyn Szadkowski 5/2005, s.71
[18]. Mikroelektrownie i małe elektrownie wodne Kompletny podręcznik odbudowy, [w:] http://trmew.pl/index.php?id=podrcznik
[19]. Niechciał J., Energetyka wodna. Polska wobec świata, Energia Gigawat 9/2014, s. 4
[20]. Rosik-Dulewska Cz. Wiatkowski M.,: Stan obecny i możliwości rozwoju energetyki wodnej w województwie opolskim, Woda-Środowisko-Obszary Wiejskie 2(38)/2012, s. 314
[21]. Solski W., Małe elektrownie wodne – warto cenić wartość, Biuletyn Stowarzyszenia Rzeczoznawców Majątkowych Województwa Wielkopolskiego 1/2012, s. 29

[22]. Thier A., Kwestia deficytu zasobów wodnych na świecie, Studia i Prace WNEiZ US 46(1)/2016, s. 184
[23]. Ustawa z dnia 20 lipca 2017 r. - Prawo wodne (Dz.U. 2017 poz. 1566)
[24]. Wesołowska H., Młynarstwo wiejskie Opolszczyzny od XVIII do XX w, Instytut Śląski, Opole 1969
[25]. www.agroenergetyka.pl
[26]. www.cire.pl/item,38932,2,0,0,0,0,0,polityka-energetyczna-polski-do-2030-roku.html Polityka energetyczna Polski do 2030
[27]. https://cink-hydro-energy.com/en/2-cell-crossflow-turbine/
[28]. www.eko.pomyslodalnia.pl/energia-wodna/(22.08.2018)
[29]. www.darmowaenergia.eko.org.pl/pliki/woda/mlyn_wodny.html/(30.07.2018)
[30]. www.energetyka.wnp.pl/w-2017-r-ponizej-50-proc-krajowej-produkcji-pradu-z-elektrowni-zawodowych-na-wegiel-kamienny,315281_1_0_1.html(29.07.2018)
[31]. www.ec.europa.eu/eurostat/statistics-explained/index.php?title=Renewable_energy_statistics/pl(30.07.2018)
[32]. www.fundacjaenergia.pl/baza-wiedzy/technologie/energia-wod/kolo-wodne(21.08.2018);
[33]. www.instsani.pl/395/historia-energetyki-wodnej21.08.2018)
[34]. www.instsani.pl/443/turbina-peltona
[35]. www.mew24.pl/wiadomosci/pokaz/5,turbina-peltona-budowa-i-zasada-dzialania
[36]. www.mew24.pl/wiadomosci/pokaz/2,turbina-banki-michella-budowa-i-zasada-dzialania
[37]. www.odnawialne-firmy.pl/wiadomosci/pokaz/101,turbina-kaplana-budowa-i-zasada-dzialania
[38]. www.odnawialne-firmy.pl/wiadomosci/pokaz/101,turbina-kaplana-budowa-i-zasada-dzialania
[39]. www.pinterest.com.mxpin/652036852283518961/
[40]. www.portalrsi.it.kielce.pl/pl/top/potencjal_hydroenergetyczny_i_je? (31.07.2018)
[41]. www.uwm.edu.pl/kolektory/turbiny-wodne/turbiny_peltona.html
[42]. www.uwm.edu.pl/kolektory/turbiny-wodne/turbiny_banki_michella.html